PURDUE UNIVERSITY
GRADUATE SCHOOL
Thesis/Dissertation Acceptance

This is to certify that the thesis/dissertation prepared

By Maia P. Kirk

Entitled

THE ROLE OF RETINOIDS IN THE REGENERATION OF THE AXOLOTL SPINAL CORD

For the degree of Master of Science

Is approved by the final examining committee:

Dr. Ellen A.G. Chernoff
Chair

Dr. Teri Belecky-Adams
Co-chair

Dr. A.J. Baucum II
Co-chair

To the best of my knowledge and as understood by the student in the Thesis/Dissertation Agreement, Publication Delay, and Certification Disclaimer (Graduate School Form 32), this thesis/dissertation adheres to the provisions of Purdue University's "Policy of Integrity in Research" and the use of copyright material.

Approved by Major Professor(s): Dr. Ellen A.G. Chernoff

Approved by: Dr. Simon J. Atkinson 7/13/2015

Head of the Departmental Graduate Program Date

THE ROLE OF RETINOIDS IN THE REGENERATION OF THE AXOLOTL SPINAL CORD

A Thesis

Submitted to the Faculty

of

Purdue University

by

Maia P. Kirk

In Partial Fulfillment of the

Requirements for the Degree

of

Master of Science

August 2015

Purdue University

Indianapolis, Indiana

For all of the loved ones in my life

ACKNOWLEDGEMENTS

I would like to thank: my advisor, Dr. Ellen A.G. Chernoff, for all of her assistance, expertise, and mentorship during the course of my Master's study; my thesis committee members, Drs Teri Belecky-Adams and A.J. Baucum for their input and review of my project; my colleagues Sarah Scott, Deborah Sarria, and Hai Nguyen for all of their protocol assistance and data contributions; and finally, I would like to thank all of my colleagues, friends, family, and most importantly, God for the support I have received and success I have experienced in the duration of this program.

TABLE OF CONTENTS

Page

LIST OF TABLES

LIST OF FIGURES

ABSTRACT

Kirk, Maia P. M.S., Purdue University. August 2015. The Role of Retinoids in the Regeneration of the Axolotl Spinal Cord. Major Professor: Ellen A.G. Chernoff

Retinoids play an important role in tissue patterning during development as well as in epithelial formation and health. In the mammalian central nervous system, the meninges are a source of retinoids for brain tissue. Retinoid production has been described in juvenile Axolotl ependymal cells. Retinoid effects may possess a significant role in the regeneration-permissive interaction of the meninges and ependyma of the Axolotl spinal cord after penetrating injury. During spinal cord regeneration in urodele amphibians, the pattern of retinoid production changes as the meninges interact with the injury-reactive ependymal cells reconstructing the injured spinal cord. In order to determine which components of the retinoid metabolism and intracellular signaling pathway act in Urodele spinal cord regeneration, we employed antibody/horseradish peroxidase staining of both intact and regenerating Axolotl spinal cord tissues obtained from adult animals as well as cell culture techniques to determine expression of three retinoid pathway components: Cellular Retinoic Acid Binding Protein II (CRABP 2), Cellular Retinol Binding Protein I (CRBP 1), and Retinaldehyde Dehydrogenase II (RALDH 2). Current results demonstrate the following in the intact cord: 1) CRBP 1 is expressed in the pia and dura mater meningeal layers, in gray matter neurons (including their axonal processes), and the ependymal cell radial processes that produce the glia limitans, 2) CRABP 2 is expressed in the arachnoid and/or dura mater meningeal layers surrounding the spinal cord, and 3) RALDH 2 is expressed in the meninges as well as

cytoplasm of grey matter neurons and some ependymal/sub-ependymal cells. In the regenerating cord, CRBP 1 is expressed in ependymal cells that are undergoing epithelial-to-mesenchymal transition (EMT), as is CRABP 2. RALDH 2 staining is very strong in the reactive meninges; in addition, expression is also upregulated in the cytoplasmic and perinuclear regions of reactive grey matter neurons, including motor neurons and in the apical region of ependymal. Preliminary studies culturing reactive meninges and ependymal cells together suggested that the meninges could drive re-epithelialization of the reactive ependymal cells. Experiments to characterize this interaction show an unusual proliferation pattern: Proliferating Cell Nuclear Antigen (PCNA) labeling is present in intact and regenerating cord ependymal cells. However, in culture, the presence of meninges results in no proliferation proximal to the explant, but extensive proliferation in leading cell outgrowth; also, the cultured meninges is positive for RALDH2. In summary, the intact adult cord shows meningeal production of RA, which is upregulated following injury; in addition, during this time, RA production is upregulated in the adult ependymal cells as well. In culture, the reactive meninges appears to modulate the behavior of reactive ependymal cells.

CHAPTER 1. INTRODUCTION

1.1 Overview

Presently in the United States, roughly 300,000 individuals suffer from some form of debilitating spinal cord injury, the most common being a crush injury-resulting from a motor vehicle accident [1, 2]. Individuals involved in military combat or civil unrest often suffer from penetrating spinal cord injuries, usually as a result of bullet, knife, or shrapnel wounds [3, 4]. Unfortunately, these penetrating spinal cord injuries usually possess the poorest outcome for recovery. Although therapies currently exist for treating severe spinal cord injuries-including drugs, stem cell applications, implanted materials as well as electrical stimulation to the injury site-they have proven to be insufficient in completely rectifying the severity of insult [1]. The principal obstacle that many clinicians and researchers face while attempting to treat penetrating spinal cord injuries is that the mammalian injury response involves the three layered meninges surrounding the spinal cord undergoing epithelial-to-mesenchymal transition (EMT) and interacting with underlying glial cells referred to as astrocytes. The interaction between the astrocytes and the meninges, resulting in extensive deposition of sulfated proteoglycans and collagen, will ultimately form a composite glial/meningeal scar. This scar will partially aid in physically stabilizing the remaining central nervous system (CNS) tissue as well as protect healthy tissue and neurons from being subjected to secondary damaging effects from the immune system (i.e.-inflammation). However, even though the damaged area of the CNS is isolated from the healthy tissues and neurons, there is a significant loss of functional plasticity, including axonal sprouting, reconstruction of

dendrites as well as modifications in neuronal activity [5]. Consequently, the injured axons will not only remain disconnected, but also engage in Wallerian degeneration that will facilitate loss of motor and sensory function distal to the site of injury, resulting in subsequent paralysis [1].

In contrast to mammalian systems, some lower vertebrates, including the urodele amphibians (newts and salamanders), are able to fully regenerate injured spinal cord, tail, and limb tissue and neurons [6]. In particular, the Mexican salamander, *Ambystoma mexicanum*, possesses robust regenerative capacity that persists into adulthood. This persistence is due to molecular pathways that are normally activated during embryonic stages being maintained in larval and reactivated in adult stages [6]. The respective CNS injury response is suggested to involve the meninges surrounding the spinal cord as well as the ependymal cells comprising the central tissue of the spinal cord [7]. The ependymal cell response has been, and is still currently, being actively investigated: it ultimately reforms the central canal and promotes axonal outgrowth and reformation of functional contacts [1, 6, 8]. The ependymal cells reconnect the cut ends of the cord, remodel the injured tissue, as well as act as stem cells [7]. The meninges temporarily invade the lesion site, but are eventually removed, forming no permanent scar. This involves the reactive ependymal cells and macrophages and matrix metalloproteinases (MMPs) in order to clear fibrotic debris (i.e.-chondroitin sulfate proteoglycans [CSPGs]) [6, 7]. In addition, ependymal cell radial processes will reform the glia limitans, which aids in axonal outgrowth by serving as bridge-like platforms for these axons as well as dendrites to follow in association with the reformed pericordal meninges [9]. Consequently, the invasive cellular and extracellular matrix (ECM) formed in injured Urodele cord is permissive for regeneration. However, the precise details of the amphibian spinal cord injury response have yet to be elucidated: many of the components of the Urodele meninges are similar to those that form an environment that is inhibitory toward regeneration in the mammal [1, 7]; consequently, it is imperative that the mechanisms involved in the injury responses of animals that regenerate are meticulously examined, investigated, and analyzed so that these same

processes can be observed, manipulated and optimized in both mammalian spinal cord injury models as well as real-life injuries [1].

The meninges have been suggested to be a rich source of retinoids: vitamin A derivatives that serve critical roles in both development and regeneration, including differentiation, reproduction, immune and nervous system function [10-12]. Retinoids facilitate such processes by first being extracted from food by the body in the form of retinyl esters (derived from animal meat) or β-carotene (derived from plants) [10, 13]. Once extracted, these esters will be converted to retinol by retinyl ester hydrolase and subsequently be bound to cellular retinol binding protein (CRBP) [14]. Some retinol will be converted back to retinyl esters by lecithin retinol acetyltransferase and will either go into circulation in the bloodstream or be transferred to a hepatocyte and be converted back to retinol and re-bound to CRBP. Within the hepatocyte, retinol can be transferred by CRBP to a stellate cell and be converted back into a retinyl ester.

Alternatively, retinol can become bound to CRBP and translocated out of a hepatocyte where transthyretin can bind to the complex and transport it to a target cell; retinol will bind to membrane receptor STRA6 and transported inside the cell. From here, retinol will be converted via retinol dehydrogenase (RDH) to retinaldehyde, and subsequently to retinoic acid (RA) via retinaldehyde dehydrogenase (RALDH). Finally, RA will be bound by cellular retinoic acid binding protein (CRABP) and translocated into the nucleus where it will bind to a retinoic acid receptor/retinoid X receptor (RAR/RXR) or RXR/other nuclear receptor (NR) heterodimer that will interact with a retinoic acid receptor element (RARE) in the target gene promoter to promote activities such as differentiation, proliferation, and apoptosis [10, 12, 14-17]. Furthermore, RA is the active metabolite of vitamin A that acts as a morphogen via translocating to the nucleus and binding to nuclear receptors in order to modify gene expression [18].

Evidence supporting the idea that RA acts as a morphogen is demonstrated in experiments where amphibian wrists were amputated and subsequently experienced increased tissue regeneration in a RA concentration dependent manner [13, 19-31]. Overall, RA was shown to modify the positional identity of regenerating limbs:

exogenous sources of RA were posteriorizing, ventralizing, and distalizing in nature, meaning the degree of limb duplication increased with increases in RA concentration. Consequently, phenomena such as proximal-distal (PD) duplication, anteroposterior (AP) axis completion, presentation of supernumerary digit formation, as well as mirror image limb formation in the dorsal ventral (DV), PD, and AP axes were present. In the regenerating Axolotl spinal cord, preliminary data from *in vitro* experiments from the Chernoff lab has demonstrated that exogenous sources of retinoids applied to cultures containing ependymal cells/ependymoglia derived from injured axolotl spinal cord tissue stimulated mesenchymal-to-epithelial transition (MET) [32]. In addition, reactive meninges (a potential source of retinoids) co-cultured with reactive ependymal cells also facilitate re-epithelialization of those glial cells via MET. Finally, when the enzyme thrombin is applied to reactive ependymal cells in culture, they also re-epithelialized via MET, identical to the response to the retinoid application. Thus, thrombin-which stimulates release of platelet derived growth factor (PDGF)- is functioning like a growth factor in that it can bind to its respective receptor to facilitate epithelialization [33, 34].

The primary objective of this thesis project is to elucidate the source and targets of retinoid signaling in Axolotl spinal cord regeneration. The first aim is to identify in which specific meningeal layers the retinoids are expressed. The second aim is to determine when, during regeneration, the meninges are a retinoid source: temporal distribution of retinoid production. The third aim is to determine the location of retinoid expression during regeneration to examine meningeal/ependymal contact in situ: spatial information. Finally, the fourth aim is to dissect the relationship of reactive ependymal and meninges using a cell culture system to determine what the effects of meningeal contact are on ependymal behavior: this is an attempt to simplify examination of meningeal/ependymal interaction using a tissue culture model that will exclude most immune system and blood-borne factor effects. Ultimately, in order to understand the significance of the role of retinoids in Axolotl spinal cord regeneration, it is necessary to put the present studies in context with what is known about related

processes occurring in mammalian spinal cord injury and in context with what is already known about Axolotl spinal cord regeneration.

1.2 Properties of the mammalian spinal cord in the context of injury

Restoration of functional stability after traumatic SCI relies on effective regeneration of the CNS and PNS. This is dependent upon not only the endogenous properties of the cells and tissues that comprise these systems, but also those of the blood and serum factors that can efficiently access those tissues as well as their progenitior cell populations [35]. Within the mammalian CNS and PNS, multipotent precursor cells exist in highly organized locations that are permissive for maintaining functional cellular interactions as well as signaling pathways [36]. Respective areas in the CNS are characterized by features such as detailed structural organization, close interaction with vessels, and cellular diversity. With regard to cellular diversity, two major classifications of cells present within CNS and PNS niches that are critical for effective recovery from injury include stem cells and progenitor cells. The former are characterized as cells that have the ability to not only self-renew, but also to generate daughter cells that can differentiate various types of mature neural cells with no restriction to a particular cell fate, such as astrocytes, oligodendrocytes, and neurons [35, 36]. Proliferative cells in general can be classified as neuronal stem cells if 1) they form primary and secondary neurospheres in culture; 2) they differentiate into the three aforementioned neural cell types *in vitro* [35]. In contrast, the progenitor cells are characterized as cells that can also self-renew like stem cells; however, their respective daughter cells are restricted to a specific cell fate, such as oligodendrocyte precursor cells (OPCs) being restricted to differentiate into oligodendrocytes [35, 36]. Stem cell approaches for treating penetrating spinal cord injuries are often desired as these pluripotent cells can potentially give rise to the cell types necessary to replace the

damaged structures and thus repair the cord. However, numerous technical, safety, and ethical constraints are present that make the use of embryonic and induced pluripotent stem cells unpredictable and inefficient for developing effective therapeutics [35]. Consequently, methods that modulate the properties of endogenous stem and progenitor cells are currently more favored.

The general structure of the mammalian spinal cord consists of a central canal lined with ependymal cells. Ependymal cells are glial cells responsible for supporting endocrine and protective functions within the central canal [36, 37]. During mammalian development the ependymal cells also possess radial processes that make contact with the basement membrane to produce the glia limitans, but during the course of development, these cells lose respective contact [38]. Adjacent to the central canal is the grey matter, which contains the cell bodies of not only neurons, but also support cells (including oligodendrocytes and astrocytes) and blood vessels [39]. Superficial to the grey matter exists the white matter of the cord, which contains long range axon tracts that are myelinated by oligodendrocyte processes [2]. In the mature mammalian cord, the endfoot processes derived from fibrous astrocytes make contact with the basement membrane to form the glia limitans. The glia limitans is critical for maintenance of the blood/CNS barrier; in addition, the fibrous astrocytes that aid in the composition of the glia limitans are important for ion, water, and neurotransmitter uptake from the extracellular milieu, which is necessary for adequate functioning of the CNS. Finally, superficial to the white matter exists the meninges. The meninges serves to protect the spinal cord from injury, composed of three layers: the pia mater (inner most layer, anchored by the pial endfeet of astrocytes), the arachnoid mater (middle layer, contains epithelial and fibrous layers), and the dura mater (outer most layer, a thick fibrous structure with a thinner cellular layer) [2, 39, 40]. Finally, bilateral denticulate ligaments extend from the pia mater to the dura mater in order to suspend the spinal cord so that it is completely surrounded by CSF and the sub-arachnoid space [39].

In mammals as well as lower vertebrates, the PNS possesses a more robust regenerative capacity than the CNS [41]. A key factor that contributes to the lack of

reformation of functional contacts within the CNS is the barrier formed by extracellular matrix (ECM) rich chondroitin sulfate proteoglycans (CSPGs) and fibrous astrocytes interacting at the CNS/PNS interface within the injury site [1, 41, 42]. Consequently, due to the inhibitory nature of the astrocyte/ECM scar, regenerating axons are deterred from continuing their outgrowth initiated by Schwann cells. In response to an environmental perturbation (i.e.-stab wound), the meninges surrounding the spinal cord undergoes epithelial-to-mesenchymal transition (EMT) and directs the action of underlying astrocytes. These astrocytes are characterized by their expression of glial fibrilary acidic protein (GFAP), a protein that is expressed in epithelium-associated intermediate filaments (IFs) of both fibrous astrocytes, ependymal glia surrounding the central canal, as well as in a small group of stem cells [7, 43]. Furthermore, both the meninges and astrocytes will then invade the lesion site to facilitate "repair" in the form of a scar [1]. The interaction between the astrocytes and meninges will ultimately form a composite glial/meningeal scar that will aid in stabilizing the central nervous system (CNS) as well as protecting healthy components from being subjected to secondary damaging effects from the immune system, including excitotoxicity, cholesterol depletion via the arachidonic acid pathway, and secondary cell death [44]. Unfortunately, at the expense of protecting healthy neurons and tissue, axons are prevented from reforming functional contacts due to the presence of scar components that are inhibitory to regeneration. In an experiment where the effects of both glial scar formation as well as axonal outgrowth were being investigated, Diaz Quiroz et al (2014) performed spinal cord transections on rats and treated them with a mimic of the mature form of miR-125b: a miRNA conserved between axolotls and mammals that is essential for functional recovery, specifically by aiding in axon growth cone repulsion/guidance via its downstream target, Sema4D (a semaphorin: a repulsive axon growth cone guidance molecule [45]), in axolotls [1]. Seven days post injury, not only were levels of Sema4D downregulated in these rats, but also those that had significant motor recovery scores according the Basso, Beattie, and Bresnahan (BBB) scoring method of locomotive ability demonstrated significant downregulation in the expression

of GFAP as well as decrease in the size of the GFAP positive scar. In addition, the quantity and size of axons projecting into the scar was greatly increased. Therefore, the presence of a glial scar composed of GFAP-positive astrocytes presents a significant barrier toward effective CNS regeneration.

Fibroblasts that comprise the meninges are the main non-neural cell type that infiltrates the lesion core to form the fibrotic component of the composite scar [45]. The most prevalent molecules present in the fibrotic scar include those that are permissive for as well as inhibitory to axonal outgrowth. Permissive molecules include collagens, laminin (LN), hyaluronic acid, and fibronectin (FN). Inhibitory molecules that deter axonal outgrowth in order to effectively isolate the area of damage (of primary interest for purposes of increasing the regenerative capabilities of the mammalian CNS) include semaphorins and various proteoglycans (notably CSPGs), both of which often produced by fibroblasts [45]. Like semaphorins, CSPGs are also involved in growth cone guidance as they possess glycosaminoglycan (GAG) side chains that constrain axonal outgrowth [45, 46]. Examples of CSPGs with the aforementioned spatial characteristics include phosphacan, versican, and NG2, which are present in the basement membrane of the meningeal epithelium and are often associated with pericytes (which are derived from blood vessels), OPCs, inflammatory and meningeal cells, as well as myelinating Schwann cells [45]. Iseki et al (2012) investigate parallel expression of the CREB/ATF transcription factor family member OASIS gene and CSPG core proteins, which are both upregulated during gliosis after CNS injury [47]. Utilizing in situ hybridization to double label OASIS simultaneously with various CSPGs (versican, brevican, neurocan, and NG2 proteoglycan cores) in cryo-injured mice brains, the authors determined that OASIS is likely upregulated in reactive astrocytes that express these CSPGs, suggesting that OASIS possesses a role in inhibition of outgrowth within the lesion core. When OASIS was transfected into competent C6 cells, the isolated membrane fraction was found to inhibit outgrowth of NG108-15 cells (neuroblastoma/glioma hybrid cell line). When chondroitinase ABC was applied to the C6 membrane fraction/NG108-15 cell line culture, the inhibitory effect previously observed was eliminated. Furthermore, being

able to effectively modulate and/or downregulate the expression of molecules refractive toward regeneration is imperative toward improving the regenerative capacity of the mammalian CNS [5].

A number of the injury responses and materials produced in the Axolotl lesion site are similar to those produced in mammal, with a very different regenerative outcome. What is known about the similarities and differences in the Urodele lesion site will be reviewed in the next section.

1.3 Properties of the axolotl spinal cord in the context of injury

In contrast to mammals, Urodele amphibians (including the axolotl) are the only tetrapod vertebrates that possess a significantly robust CNS regenerative potential [6]. The structure of the axolotl spinal cord is very similar to that of the mammal; however, the ependymal cells lining the central canal of the spinal cord possess regenerative roles instead of just those related to protection and the endocrine system [37]. One major difference is that amphibian ependymal cells possess pial endfeet that not only ultimately terminate on the basement membrane to produce the glia limitans, but also assist in the formation of the blood/CNS barrier [6, 38]. In response to injury, the meninges surrounding the spinal cord will interact with these ependymal cells (instead of astrocytes) when they invade the lesion site; ultimately, these ependymal cells will collaborate with macrophages as well as MMPs in order to clear the injury site of fibrotic debris and thus remodel the cord in a manner that is actually permissive for axonal outgrowth [1, 6]. Previous studies that have examined pre-and post-lesion levels of vimentin, GFAP, CSPGs, and collagens have supported the determination that no evidence of a glial scar is present in axolotls due to the fact that few/no fibrous astrocytes are present; in this manner, CSPGs, which have an inhibitory role in mammals, are suggested to serve a relatively permissive role in the axolotl injury

response [1]. Furthermore, possible mechanisms of action by the ependymal cells include removal of myelin, phagocytosis of resulting cellular debris, production of trophic substances that support neuron survival, and most importantly, remodeling of the ECM in a manner that is permissive for axonal outgrowth [38]. Ultimately, the ependymal cells at the caudal end of the lesion will migrate to seal off the lumen of the spinal cord by forming a bulb around the damaged end of the cord; ependymal mesenchymal outgrowth rostral to this area will extend and form an ependymal tube [15]. In the axolotl, there is mesenchymal ependymal outgrowth from the rostral and caudal stumps which meets and reforms a solid ependymal bridge that ultimately reforms an ependymal tube [6, 43]. Finally, stem cells generated from these ependymal cells will proceed to differentiate into CNS neurons, glia, and peripheral ganglia in order to restore CNS function: axons and dendrites will grow either in between pial endfeet or processes in close contact with the basal lamina [9]. Moreover, the robust regenerative capacity seen in axolotls is incomparably attributed to the ependymal cells organizing themselves so that they can seal the lesion, re-extend their pial endfeet to produce a new glia limitans, and allow space to exist between themselves and their glia limitans so that axons can actually traverse through the lesion core.

O'Hara et al (1992) characterized EMT of injury reactive ependymal cells in situ by harvesting transected spinal cord tissue from juvenile and adult axolotls at various post-lesioning time points. They not only observed the morphological changes of the regenerating tissue, but also analyzed the changes in various markers of tissue, including IFs such as cytokeratins, vimentin, GFAP, and the ECM component fibronectin (FN) [43]. By two weeks post-lesioning, the cranial and caudal ends of the cord had made contact with each other, as confirmed by stereomicroscopic examination and histology; by three week post-lesioning, the mesenchymal outgrowth had fused the cranial and caudal stumps; finally, by four weeks post-lesioning, the ependymal cells surrounding the central canal had undergone MET and reformed an epithelium; in addition, newly myelinated axons were present. Overall, morphological analysis of regenerating axolotl

spinal cord tissue indicated that EMT of injury reactive cells was present in order to aid in remodeling the cord (reviewed in [6]).

Immunohistochemistry (IHC) of frozen spinal sections derived from one to six week regenerates was employed using fluorescence microscopy to target expression of the aforementioned markers. Expression of cytokeratins was present in apical ependymal cells of the un-injured axolotl cord; however, respective expression was downregulated for two to three weeks post-lesioning. Instead, vimentin was upregulated during this time period, indicating that the injury reactive cells were becoming mesenchymal in nature. In addition, both were co-expressed for a one to two week period, which indicated that EMT was occurring.

GFAP was down-regulated one week post-lesioning in the ependymal radial processes and subsequently upregulated four weeks post-lesioning (coincident with the time newly myelinated axons appear). Finally, FN was up-regulated during mesenchymal ependymal outgrowth two to three weeks post lesion (closely following the appearance of vimentin during mesenchymal cell migration) and down-regulated five week post-lesioning (when the ependymal cells had re-epithelialized around the central canal). Moreover, the expression patterns of these markers during the in situ tissue examination highlight the spatial and temporal characteristics of injury reactive ependymal cells: these cells undergo EMT, followed by MET, to manipulate the cytoskeleton in order to modify cell shape, change levels of ECM production, and tissue organization so that the lesion can be repaired and axonal outgrowth can proceed. Fluorescent labeling of the cytoskeleton in cell cultures comprised of ependymal cell explants plated on poly-D-Lysine/FN coated dishes was employed by utilizing rhodamine-phalloidin staining of actin filaments in order to determine if the outgrowth from these explants was epithelial or mesenchymal. After six days, the ependymal cells exhibited an elongated morphology oriented outward as they migrated away from the explant as well as a lack of epithelial organization. After 16 days, actin microfilaments bundles were observed to be oriented along the long axis of the cells. In addition, there was an absence of apicobasal polarity, which is suggestive of a cell that is mesenchymal

in nature; this morphology persisted for periods of up to six weeks. Correspondingly, two week regenerate ependymal cell explants examined at 10-16 days after placement in culture not only expressed vimentin and lost cytokeratins, but also adhered to the FN substrate, indicating that the explant cells were migrating and then re-epithelializing. Furthermore, ependymal cells were found only to re-epithelialize in response to thrombin or retinoids: If simply provided with EGF (a powerful stimulant of EMT), the cells would remain mesenchymal [32]. Thus, the results obtained from the *in vitro* cell culture experiments suggests that a functional relationship exists between the intermediate filament and ECM responses that modulate the axolotl spinal cord injury response. Altogether, both the *in vitro* and in situ work supports the idea that the ependymal cells indeed migrate into the lesion site and interact with overlying meningeal cells to close off spinal cord lesions in a manner that allows for axons to traverse the lesion core, reform functional contacts, and restore functional stability in the axolotl CNS.

With both similarities and differences in the mammalian and urodele spinal cord lesion responses, the next question is whether retinoids, important in spinal cord development in mammals, are important in mammalian spinal cord health or injury, discussed in the next section.

1.4 Retinoid Metabolism

With regard to retinoid action in the context of mammalian and Urodele amphibian physiology, the most common circulating forms of retinoids include retinyl esters (a storage form of vitamin A), retinol, retinal (retinaldehyde), and RA [48]. Their respective metabolism in the body involves a class of proteins that act in the cytoplasm as well as a class of proteins that act in the nucleus [49]. The former include CRBP (also called RBP) and CRABP, while the latter include the RAR and RXR receptor families.

Generally, retinoids are either associated with a cellular membrane or bound to a specific retinoid binding protein. Vitamin A is primarily transported either as retinyl esters present in lipoproteins or as retinol bound to a specific CRBP [10]. Retinyl esters are stored in the liver; after being converted to retinol, CRBP will bind it and deliver it to either an alcohol or a retinol dehydrogenase (RDH) [10, 11]. The dehydrogenase will convert retinol to retinal, and its respective dehydrogenase (RALDH) will convert retinal to RA. Finally, CRABP will bind RA, translocate it into the nucleus, and form a complex with either a RAR/RXR or a RXR/NR heterodimer so that RA can modify gene expression and promote regenerative activities [10, 11, 14, 50].

The cellular binding proteins CRBP and CRABP essentially function to move the specific retinoid metabolite to its cellular target: CRBP not only inserts retinol through the plasma membrane by binding to membrane receptor STRA6, but it also keeps retinoids soluble and stable within aqueous spaces [14]. CRBP has been shown to localize to the ventral floor plate of developing organisms, which contain radial glia [19, 49]. Radial glia have processes that traverse the white matter to the periphery of the spinal cord and take part in activities such as patterning, neuronal migration, and neurogenesis [49]. Furthermore, in urodele amphibians, CRBP 1 is also found in the ependymal cells surrounding the spinal cord; together with other glial cells, these CRBP-positive ependymal cells may function to concentrate retinol, metabolize it to RA, and release it so that neurite outgrowth from existing neurons in the proximal environment may proceed [25, 41, 49].

CRABP is suggested to possess a role in axon maintenance, corroborating with the observation that cellular levels of RA need to be closely regulated [49]. It is expressed in white matter axons as well as commissural axons extending across the ventral floor plate [19, 25, 49, 51]; In the axolotl, essentially all axons are CRABP-positive [25]. With respect to limb bud development, graded expression is present: downregulation of CRABP has been demonstrated to inflict mild effects on proper maturation of limbs [14, 27]. Ultimately, its primary role is to ensure RA arrives to the nucleus so that it can modify gene expression via forming complexes with the

aforementioned nuclear receptor heterodimers; however, in the presence of these receptors, CRABP is not required for RA-dependent gene activation [50]. Nevertheless, CRABP plays a pivotal role in the morphogenic nature of RA and thus in the regeneration process.

Cellular RA is present in two active isoforms: all-trans RA (ATRA) and 13-cis-RA [10]. However, ATRA is the most physiologically important form of vitamin A in the body; it accounts for 99% of all forms of all vitamin A present [48]. Additionally, CRABP has been shown to possess a high affinity for ATRA over 13-cis-RA[14]. Zhang et al (2003) highlight this physiological importance by demonstrating that the meninges is a rich source of RA for the late-developing mammalian hindbrain [12]. Utilizing tissue from *RAREhsplacZ* RA reporter mice that were developed for β-galactosidase, in situ hybridization was performed on whole mounts and sections using probes for cytochrome P450, family 26, subfamily B, phenotype 1 (CYP26B1, enzyme that catabolizes RA) and CRABP 1. In addition, E12 and E14 hindbrain explants were cultured and had their meninges removed for subsequent use in antibody labelling for RALDH 2 and β-galactosidase. Overall results indicate not only that RALDH 2 was predominantly expressed in the meninges surrounding the brain, but also that CYP26B1 was enriched in the anterior ventricular surface and in several hindbrain nuclei. In addition, CRABP 1 was present in all precerebellar neurons that migrate under the meninges. RA concentration assay results indicate that meningeal hindbrain and SC tissue released large amounts of RA into the medium, with the highest levels being present in the meninges around the cerebellum. Finally, culture explant results indicate that if the meninges is removed at E12, there is an absence of RAREhsplacZ positive neurons; expression is upregulated if 10nM RA is added to the serum-free medium. However, if the above is performed at E14, exogenous RA will not re-induce expression as the developmental process is at too late of a stage for vitamin A to be able to exert effects; thus, RA must be derived from the meninges to induce the reporter. Overall, these results posit that patterning exhibited by RALDH 2 concurrent with the localization of the RA response reflect RA signaling in the hindbrain that predominately occurs around its peripheries, most

notably in precerebellar neurons migrating around the hindbrain circumference that form pontine nuclei; with regard to CYP26B1, being that it is expressed in the subregions of the ventricular wall as well as in deeper regions of the hindbrain (in/around developing nuclei), its role in hindbrain development may be to protect those regions from RA influence. Consequently, discrete concentrations of RA in the hindbrain are necessary to deter teratogenic developmental effects.

The RAR family of nuclear receptors RARs is a part of the steroid/thyroid hormone receptor superfamily that serves to transduce the RA signal at the genomic level [25]. By forming heterodimers with RA and RXRs, they will undergo a conformational change will facilitate the recruitment of co-activators and co-repressors and bind RAREs that are upstream of the target gene in order to repress or activate gene expression [15-17, 52]; in the absence of an activating ligand, RAR/RXR heterodimers are proposed to be bound to DNA [16]. The co-regulatory complexes integrate info from external signaling events: they facilitate communication between mediator and basal transcription complexes as well as by remodeling chromatin.

The RAREs usually consist of two direct repeat half-site consensus sequences of AGGTCA [52]. Elements that have the direct repeats spaced by 5bp (DR + 5 element) facilitate the heterodimers to bind upstream of the half-site and activate transcription in response to RAR-specific ligands (i.e.-RA). In contrast, response elements that possess direct repeats spaced by 1 bp (DR + 1 element) facilitate the heterodimers to bind to the downstream half-site in order to repress RXR-dependent transcription. Furthermore, if the polarities of the binding interactions are reversed (i.e.-a heterodimer complex binding downstream-rather than upstream-of an RARE possessing a DR+5 element), the transcriptional responses are reversed as well. Theodosiou et al (2007) demonstrate how upregulation of neural proliferation, differentiation and control (NPDC-1) protein during late axolotl embryogenesis correlates with a reduction of proliferation as well as RAR-mediated transcription[16]. Previous work done by these authors highlights that mammalian NPDC-1 functions as a retinoid receptor co-repressor *in vitro* by binding directly to retinoid receptor family members to inhibit respective binding and

consequently repressing respective mediated transcription. In the axolotl, NPDC-1 exhibits maximal expression during limb development, which is modulated by RA-signaling. Furthermore, the encompassing results indicate that axolotl NPDC-1 was differentially expressed among multiple tissues during development, predominantly in the heart, brain, eye, skin and gill. Co-expression of RARγ and NPDC-1 was also observed, especially in the heart. In addition, a pull-down assay and EMSA confirm that RARγ and NPDC-1 interact to form a complex. Finally, the *in vitro* cell transfection results demonstrate that this NPDC-1 indeed interacts with RARγ and inhibits its binding to DNA, ultimately repressing RARγ mediated transcription and cell proliferation. Moreover, modifications that reduce the efficiency of the RA pathway in both the mammal and the axolotl can have detrimental consequences on development [16].

Kern et al (2007) demonstrate that expression of RALDH 2 in rat meninges increases after spinal cord contusion injury, most notably in the arachnoid [53]. Quantitation of expression levels via Western Blot analysis revealed that tissue extracts derived from lesioned animals consistently displayed higher protein levels of RALDH2 compared (relative immunoreactivity values of 1.6, 1.4, and 1.3 for 4, 7, and 21 dpo, respectively) to sham-operated animals (relative immunoreactivity value of 1.0). IF labeling of spinal cord tissue sections also revealed increases in immunoreactivity of RALDH 2 21 dpo, specifically around blood vessels, within cells, and in the meninges associated with the lesion site. Within the lesion core, meningeal staining of RALDH 2 was more prominent and also present within more layers of cells; in addition, reactivity was observed in NG2/RALDH 2-positive cells that were located between the spinal cord surface (where the meninges are located) and the lesion site, suggesting that these cells migrated from either the pia or arachnoid. However, since RALDH 2 was also expressed around blood vessels (which are highly abundant in the arachnoid), the data support the suggestion that the origin of these NG2/RALDH 2-positive cells is from the latter layer.

Hunter et al (1991) utilized immunocytochemical methods to target localization of CRABP and CRBP within axolotl spinal cords[49]. Respective antibodies applied to cord sections derived from 4-8cm juvenile axolotls targeted expression of CRBP

primarily in radial glial cell bodies of the gray matter; conversely, CRABP was notably present in white matter axons (i.e.-those derived from radial glia). Furthermore, Western Blotting performed with axolotl brain and spinal cord tissue confirmed that the two cytoplasmic binding proteins did not cross-react with eachother-each protein generated bands of distinct sizes, with that for CRBP having a size corresponding with that of rat pure CRBP (approximately 15 kDa). Furthermore, both the mammalian and axolotl CNS demonstrate evidence RA production based upon the presence of RA synthesizing and binding proteins, respectively, found in cord and tissue samples.

As retinoids have been shown to be present in mammalian and axolotl spinal cord tissue and have demonstrated to be actively involved in the respective injury response, it is imperative to consider the resulting effects of inhibiting components of the RA pathway, which will be discussed in the proceeding section.

1.5 RA inhibitors and their effect on tissue regeneration

Investigating the effects of inhibition of retinoid metabolism is essential for qualifying the effects of retinoids on mammalian and Axolotl spinal cord tissue regeneration. Several inhibitors have been studied and shown to be effective in negatively affecting metabolism. In future studies inhibitors will be used to determine the specific involvement of retinoids in ependymal/meningeal interactions.

Disulphiram has been shown to inhibit axolotl limb regeneration by antagonizing aldehyde dehydrogenases (including RALDH) in a non-discriminatory manner [30, 54]. When applied to mouse, chick, rat, zebrafish retina, and chick limb buds at low micromolar concentrations, outgrowth was inhibited. Similarly, citral has been shown to inhibit RA synthesis by antagonizing RDH and RALDH [51, 54]. Scadding (1999) demonstrates that after treatment of regenerating forelimbs of larval axolotls, citral inhibited caused the limbs to be hypomorphic, coinciding with various pattern defects,

including digit fusion, reduction in digit numbers, and reduction in the length of the radius and ulna [54]. In addition, Tanaka et al (1996) highlight that in a chick wing bud organ culture system derived from stage 19/20 embryos, citral facilitated an abnormal patterning defect on distal wing structures (radius and ulna), which were less specified at that point in time compared to more proximal structures (humerus) [51]. These authors also comment that application of exogenous RA and citral in combination should rescue the induced patterning defect since both cause teratogenic effects individually. Furthermore, Johnson and Scadding (1992) demonstrate that via intraperitoneal injection of RA, followed by exposure to tunicamycin, amputated axolotls did not exhibit the proximalizing regenerative effects of RA [24]. Tunicamycin is an antibiotic that blocks glycosylation of proteins at aspartate residues, thus interfering with adhesivity as well as morphogenetic movements during various stages of amphibian development. Consequently, if tunicamycin blocks the proximalizing nature of RA, then it is likely that glycoproteins are important participants in the reaction sequence modulated by RA.

Del Rincón et al (2002) also demonstrate that various retinoid antagonists were able to inhibit normal patterning during limb regeneration to various extents [29]. However, rather than use inhibitors such as disulfiram and citral, the authors tested specific inhibitors of RA metabolism as they were concerned that lack of specificity of action executed by disulfiram and citral may influence regeneration in ways other than simply blocking the synthesis of RA: their targets, alcohol and aldehyde dehydogneases, can act on substrates other than retinoids. Inhibitors tested include: Ro41-5253 (RARα selective), Ro61-8431 (RARα, β, ϒ specific; pan antagonist), LE135 (RARβ selective), and LE540 (binds to all RARs and RXRs; pan antagonist). After implanting silastin blocks (that released varying concentrations of ATRA and/or the aforementioned antagonists in a slow and effective manner) into the limbs of amputated axolotls, the limbs that received administration of both ATRA and either Ro41 or Ro61 displayed no noticeable difference in effect: all limbs showed missing/incomplete development of phalanges as well as reduced density. General inhibition of regeneration was exhibited when LE135 was

implanted individually; in contrast, the majority of limbs implanted with LE540 silastin blocks appeared like the controls. Limbs implanted with silastin (silicone elastomer) blocks containing LE135 and LE540 revealed partial regeneration, indicating that a balanced inhibition of all RARs may be less disruptive to patterning compared to inhibition of a select subtype. Furthermore, the effects of RARα antagonist Ro41 were less detrimental than those of RARβ antagonist LE135; thus, the former may be dispensable for regenerating limb patterning. In conclusion, although there are numerous inhibitors of RA metabolism, ones that are specific for individual retinoid subtypes in the pathway-rather generic dehydrogenases that act upon those subtypes-will be more accurate for determining the detrimental effects of downregulating the RA pathway in the context of regeneration. Moreover, my future PhD studies will pursue the use of LE135 and LE540 *in vivo* and *in vitro* to examine changes in expression of RA pathway proteins as well as those of ependymal tissue re-epithelialization, respectively. Ultimately, these objectives of my PhD research will aid in further elucidating the effect of retinoids on spinal cord regeneration.

CHAPTER 2. MATERIALS AND METHODS

2.1 Animal Source

Sub-adult wild type axolotls were obtained from the University of Kentucky Ambystoma Genetic Stock Center (AGSC) in Lexington, KY. The animals were maintained in plastic tubs containing room temperature 1x Holtfreter's solution under the care of veterinary technicians in the Indiana University-Purdue University-Indianapolis Science Animal Resource Center (SARC) until ready for use in transection surgeries.

2.2 Transection Surgeries

All axolotls were allowed to mature to adult stage before being utilized for research. After sterilizing workbenches and materials under UV lighting for 15 minutes, axolotls were first anesthetized in 0.75g/L Tricaine Methanesulfonate solution (Finquil; Western Chemical Company, Ferndale, WA), pH 7.4, supplemented with thimerosal as an antiseptic for approximately 45 min; prior to surgery, animals were tested for the absence of reflexes to ensure the proper level of anesthesia was achieved. Next, animals were placed on their sides and surgical scissors were used to cut a one inch flap just above the cauda equina (to avoid paralyzing the bladder). While frequently rinsing with Hank's Balanced Salt Solution (HBSS) containing [1:100] penicillin/streptomycin/ fungizone (PSF), the underlying muscle and fat were removed with electronic grade

forceps until the spinal cord vertebrae were exposed; this bone was subsequently removed to expose the spinal cord. Microscissors were used to completely transect the spinal cord. Finally, the lesion site was re-covered with the skin flap and the animals were placed in chilled 1x Holtfreter's solution until the animals recovered from the effects of anesthesia (approximately 45 minutes); the animals were then placed in plastic tubs filled with chilled 1x Holtfreter's solution and transferred to a Biochemical Oxygen Demand (BOD) incubator set at 12 degrees Celsius.

2.3 Axolotl Spinal Cord Tissue Harvest

Lesioned axolotls were allowed to regenerate for two to five weeks: the first length of time proved to be optimal for obtaining sufficient ependymal mesenchymal outgrowth before the cord completely fused back together; the second length of time shows regeneration as determined by microscopic examination and recovery of coordinated tail use in swimming. During the surgical recovery period (the first three days), animals were injected with amikacin for prophylactic treatment. In addition, they were fed both nutritional pellets (Rangen Soft Moist Pellets) and shrimp brine; Holtfreter's solution was changed daily. After this time period, animals were anesthetized and prepped for surgery as previously described; the cord/tissue was cut rostral and caudal to the lesion core and was placed in 4% paraformaldehyde (PFA). The axolotls were subsequently euthanized by transecting their cervical vertebrae and transferred to the SARC for incineration.

2.4 Immunohistochemistry: Horseradish Peroxidase (HRP) staining and fluorescent antibody labeling of paraffin embedded and whole mount tissue sections

The cord segments placed in 4% PFA and situated on a rocker until subsequent changes of PFA resulted in less drastic changes in pH; the cords were then allowed to incubate four degrees Celsius overnight in PFA. The following day, the spinal cord segments were prepped for removal of surrounding bone and subsequent embedding in paraffin wax by subjecting them to 1% Ethylenediaminetetraacetic acid (EDTA, pH 7.4) for one hour. After dissecting the cords out of the bone, they were dehydrated in a series of solvents: two changes (2x) of phosphate buffered saline (PBS) for 15 minutes each, followed by serial placement into 10%, 30%, 2 x 50%, 2 x 70%, 2 x 90%, and 2 x 100% ETOH, each for 30 minutes. The cord segments were either isolated from surrounding bone or left in bone and placed in 100% ETOH at -20 degrees Celsius until they were ready to be embedded in paraffin. At this juncture, tissue aliquoted for whole mount analysis was cut into thick sections before placement into 100% ETOH. To ensure that the spinal cords used for embedding in paraffin would be sufficiently miscible with the paraffin wax, they were placed in two changes of xylene for 45 minutes each, followed by two changes of paraffin heated to 60 degrees Celsius for 30 minutes each. The cord segments were subsequently placed in a third change of paraffin overnight and placed in molds the following day.

Paraffin embedded spinal cord segments were sectioned on a microtome (Lipshaw Manufacturing Company, Detroit, MI) at a width of ten micrometers placed onto Vectabond-coated glass slides (Vector Laboratories) and subsequently allowed to dry on a slide dryer overnight. The following day, the tissue sections were baked in a hybridization oven at 50 degrees Celsius for five hours, followed by deparaffinization in xylene and rehydration in a decreasing ETOH gradient as well as PBS. Both whole mount thick sections and paraffin thin sections of tissue were next subjected to either antibody labeling concurrent with HRP staining or fluorescent secondary antibody labeling to

identify the spatial expression patterns of five retinoid proteins: CRABP 2, CRBP 1, RARβ, RXRγ, and RALDH 2 [55]. Immunoperoxidase was used for antigen localization because the robust green autofluorescence of damaged axolotl CNS tissue could not be suppressed. Subjection to 0.01 M citric acid heat-mediated antigen retrieval at 90 degrees Celsius for 15 minutes was followed by blocking non-specific binding sites with one of the three following blocking buffers: A 1:1 ratio of [1:10] diluted normal animal serum in PBS/tween 20 (Ptx):Superblock (Pierce), a 1:1 ratio of [1:10] diluted normal animal serum in tris-buffered saline/tween 20 (TBST): Superblock, or 1x Blocking reagent (Roche; 10x stock diluted 1:10 in 1x maleic acid buffer, pH 7.5). Finally, application of the primary antibody was employed for overnight incubation at four degrees Celsius.

Tissue sections were then subjected to quenching of endogenous peroxidase with 3% hydrogen peroxide (diluted in MQ water). For HRP staining, the biotinylated secondary antibody was allowed to incubate either for one hour or overnight, followed by incubation with an avidin-biotin enzymatic complex (ABC) (Vector Laboratories) and application of the peroxidase substrate 3,3'-Diaminobenzidine (DAB) (Vector Laboratories). Lastly, the tissue sections were counterstained with Nuclear Fast Red, dehydrated with an increasing ETOH gradient and xylene, and mounted with an organic mounting medium. In contrast, for fluorescent antibody labeling, a fluorescent secondary antibody was added after the peroxidase quench and allowed to incubate for one hour in the dark, followed by mounting with 4', 6'-diamino-2-phenolindole (DAPI) anti-fade and sealing the slide with nail polish. Finally, the tissue sections were analyzed with a Nikon Eclipse E800 epifluorescence microscope.

Primary antibodies utilized for selected retinoids as well as ependymal and meningeal tissue markers were diluted in either a [1:10] dilution of normal animal serum in Ptx, a [1:10] dilution of normal animal serum in TBST, or 1x Blocking Reagent; secondary antibodies used were diluted in either Ptx, TBST, or 1x maleic acid buffer (pH 7.5). Primary and secondary antibodies and respective concentrations are listed in table 2.1.

2.5 Preparation of cell cultures containing reactive ependymal cells and meninges

Fibronectin (FN; BD biosciences) was utilized as the culture substrate for the reactive tissue at a concentration of 1mg/ml. After the FN was allowed to equilibrate at room temperature for 15 minutes, 1 ml of nuclease free water was added, followed by allowing the suspension to sit for 30 minutes. The FN was diluted to 10-11 ml with either sterile 4-(2-hydroxyethyl)-1-piperazineethanesulfonic acid (HEPES) or Hank's balanced salt solution (HBSS) and subsequently sterile filtered. 10 mm polystyrene culture dishes were coated with 1 mg/ml of poly-L-Lysine (Sigma), which were subsequently placed in a 150 mm culture dish containing a humidifier (a 10 mm culture dish containing nuclease free water) and allowed to incubate at 37 degrees Celsius for one hour. Since the polystyrene culture dishes are negatively charged, and the FN possesses an abundance of negatively charged moieties, the addition of a substrate with numerous positively charged moieties (poly-L-Lysine) prior to addition of the FN will allow it to adequately adhere to the dishes. The culture dishes were then coated with sterile FN and allowed to incubate at 37 degrees Celsius for one hour; excess FN was subsequently removed, followed by rinsing two times with sterile HEPES or HBSS. The second application of HEPES/HBSS was allowed to remain in the culture dishes. Finally, the FN coated dishes were stored at four degrees Celsius in the large 150 mm dish for up to 48 hours.

The culture dishes were then rinsed two times with sterile axolotl basal media (table 2.2) containing penicillin/streptomycin/fungizone (amphotericin B) [PSF; Cellgro]. and epidermal growth factor (EGF, stimulates tissue binding to FN), which was subsequently used as culture medium. Harvested intact or regenerate spinal cord tissue was subjected to three 10 minute washes with HBSS containing PSF.

The ependyma was subsequently separated from the meninges; both were then minced into small pieces and distributed equally between the culture dishes. The axolotl basal media was removed from the dishes and replaced with only a few drops of this

medium in order to aid in the explant adhesion process. The cultures were allowed to incubate at 21 degrees Celsius while rocking them every 20 min for two hours in order to allow the explants to sufficiently adhere to the FN. Finally, fresh medium was added after the final twenty minute interval and was changed the next day, followed by every 48 hrs.

Cultures of cleaned reactive ependymal explants were grown with no EGF or retinoid as a control. A culture containing only reactive meninges was stained with α-RALDH 2 to confirm that retinoid metabolism-upregulated during injury-is still present in culture; and finally, a co-culture of reactive meninges and ependymal cells was stained with α-CRABP 2 to confirm that the cells are capable of utilizing RA in the cultured tissues. Moreover, selected cultures were fixed overnight with 4% PFA, permeabilized with 0.01% Triton-x, and stained with Rhodamine-Phalloidin (Life Technologies) to stain actin filaments [56]. In addition, cultures subjected to antibody labeling were done so utilizing the HRP protocol (with DAPI utilized as a counterstain), following overnight fixation and subsequent permeabilization. Finally, cell cultures were photographed daily for appropriate documentation using a Nikon Eclipse TE200-U inverted microscope. A list of the cell culture experiments performed is provided in table 2.3.

2.6 Quantitation of ependymal cell proliferation

Quantifying expression of ependymal cells within non-reactive (control) as well as injury reactive ependymal cells was executed by labeling either spinal cord tissue sections or cultures with an anti-Proliferating Cell Nuclear Antigen (PCNA) antibody in order to identify ependymal cells that are mitotically active. The mitotic index (MI) was calculated by utilizing multiple sets (one set=3-4 animals) of corresponding data for both the intact and regenerate tissue sections (in situ) as well as pure ependymal and meningeal/ependymal explant tissues (*in vitro*): the MI is defined as the ratio of cells

binding DAPI (all cell nuclei) to those expressing PCNA (nuclei of proliferating cells). Data is presented as the average ± the standard error of the mean (SEM) [57].

CHAPTER 3. RESULTS AND DISCUSSION-IMMUNOHISTOCHEMISTRY PERFORMED ON AXOLOTL SPINAL CORD TISSUE SECTIONS TO STUDY THE ROLE OF RETINOIDS *IN VIVO*

3.1 Overview of use of immunohistochemical method to target expression of retinoid proteins

Employing antibody labeling with either HRP or immunofluorescence (IF) will aid in determining both the spatial and temporal expression patterns of retinoids of interest in situ. Specifically, expression of CRABP 2, CRBP 1, RARβ, RXRγ, and RALDH 2 were chosen for investigation within three types of spinal cord tissue derived from adult axolotls: intact cord, serving as an uninjured tissue control; two week regenerate cord, a time point where there is ependymal mesenchymal outgrowth; and five week regenerate cord, when a transected cord that is reconnected with reformation of a central canal. Additionally, sectioned mouse embryo tissue was used as a positive control for labeling with antibodies made against mammalian proteins (specifically α-RALDH 2, figure 3.14). Tissue subjected to peptide blocking and application of only a secondary antibody served as a staining negative control (figure 3.1). The overall staining process for both methods involves application of a primary antibody that will bind to the protein of interest [55, 58]. Moreover, both the HRP and IFs method is an excellent method for targeting protein expression as it provides spatial and temporal expression of the antigen of interest while being able to simultaneously view all aspects of the spinal cord tissue sample when bleed-through of the strong green autofluorescense of injured amphibian CNS tissue is a problem.

3.2 Intact axolotl spinal cords labeled with α-CRABP 2 and α-CRBP 1

It is imperative to note that at this point in time it cannot be determined for certain as to which distinct layer is expressing each retinoid as literature to date simply refers any respective protein expression in each the three meningeal layers as the expression being present in the meninges. Even in mammals the arachnoid and dura have species-specific differences and the identification of dura or arachnoid is made principally by assertion. There are no layer-unique markers at this time. In addition, there are regional differences (both anterior/posterior and dorsal/ventral) in the spinal cord [59, 60]. Subdivisions also appear as a result of physical forces in isolation of the meninges for analysis [59, 61]. In the intact cord, CRBP 1 was expressed in the pia (as indicated by staining on proximal aspect of denticulate ligament) and dura mater meningeal layers as well as the cytoplasm of grey matter neurons; in addition, it was localized in neuronal and ependymal cell processes (figure 3.2). In contrast, CRABP 2 was distinctly expressed in the dura and/or arachnoid meningeal layers (figure 3.3). The association of strong staining in a middle meningeal layer associated with extensive vascularization makes it likely that this layer includes the arachnoid. Although the pia is adjacent to the arachnoid, there was absence of an additional thin line of staining between the white matter and the arachnoid (e.g.-on the proximal aspect of the denticulate ligament, an extension of the pia) suggesting that the pia is negative for CRABP 2.

3.3 Regenerating axolotl spinal cords labeled with α-CRBP 1 and α-CRABP 2

All transected cords were allowed to regenerate for approximately two weeks before harvest to achieve the ependymal outgrowth stage; sections were either taken from the area of the cord in the lesion site outgrowth or from a site several millimeters

distant from the lesion, termed reactive stump tissue. Reaction to lesioning is known to extend a considerable distance from the lesion site, at least five millimeters from the cut ends [62]. Both CRBP 1 and CRABP 2 were localized in the cytoplasm of reactive apical ependymal cells that were undergoing EMT (figure 3.4); ependymal cells are easily identified by distinctive speckled appearance when subjected to nuclear fast red staining (figure 3.5), as previously characterized in our laboratory and correlated with Musashi-1 expression (i.e.-Musashi-1, a notch pathway RNA binding protein that is expressed in mesenchymal [reactive] ependymal cells [63, 64]). In stump cord sections, as in the intact cord, CRBP 1 was expressed in the processes of grey matter neurons (figure 3.6). However, there was significant upregulation of CRBP 1 in both the ependyma and grey matter neurons, unlike CRABP 2. In contrast, CRABP 2 was shown to be expressed in the dura/arachnoid, like in the intact cord (figure 3.7); interestingly, CRABP 2 expression had also been activated in the pia of the stump tissue. In addition, there was some perinuclear staining present in the ependymal cells in the reactive stump.

Both CRBP 1 and CRABP 2 were expressed in the apical cytoplasm of those ependymal cells (figure 3.8). Yet, when comparing differential expression in the meninges of these stump cords, CRABP 2 was much more strongly expressed than CRBP 1. In the five week regenerating axolotl cord, CRBP 1 and CRABP 2 both were not expressed in the ependymal cells (figures 3.9 and 3.10) and only CRABP2 is strongly expressed in the dura/arachnoid mater (figure 3.10). Overall, CRBP 1 and CRABP 2 exhibit differential expression that is dependent both on the distance from the lesion site as well as how long the tissue was allowed to regenerate; a summary of the expression patterns is provided in table 3.1 as well as in figures 3.11 and 3.12, respectively.

3.4 Intact and regenerating axolotl spinal cords labeled with nuclear receptors antibodies α-RARβ and α-RXRγ

Unfortunately, attempts of targeting expression of RARβ and RXRγ nuclear receptors within axolotl tissue were unsuccessful (figure 3.13): since both are nuclear receptors to which RA can bind, nuclear expression should be clearly evident; in addition, both have been cloned in the axolotl [31]. However, some nuclear staining for RXRγ is present within a mouse embryo (figure 3.14). Therefore, in order to further characterize expression of these nuclear receptors, polymerase chain reaction (PCR) will have to be employed using cDNA from a regenerating tissue mRNA in future studies.

3.5 Intact and regenerate axolotl spinal cord labeled with α-RALDH 2

The efficacy of α-RALDH 2 was shown by the staining present within the tissue of the positive control mouse embryo (figure 3.15). In the intact cord, expression of RALDH 2 was exhibited in the meninges as well as the cytoplasm of grey matter cells and (sub) ependymal cells (figure 3.16). The regenerating axolotl cord at the lesion site demonstrated significantly upregulated expression in the reactive meninges (figure 3.17); in addition, localization was upregulated in the cytoplasmic and perinuclear regions of reactive grey matter and apical ependymal cells. Reactive stump cord revealed results identical to those of the reactive tissue at the lesion site (figure 3.18). Finally, in a five week regenerate, RALDH 2 was found to be expressed in the meninges as well as in the cytoplasm of grey matter and apical ependymal cells (figure 3.19). A summary of RALDH 2 expression is given in table 3.1 as well as figure 3.20.

3.6 Intact and regenerating axolotl spinal cords labeled with α-Sema3A, α-hMsi-1, and α-GFAP

Sema3A was demonstrated to be expressed not only in the perinuclear and cytoplasmic regions of grey matter cells constituting the adult intact cord, but also in the pial layer of the meninges (figure 3.21). This layer is thin and very closely apposed to the basal (outer surface) of the intact cord, strongly suggesting pial identity. In full sections, the characteristic gray matter butterfly shape includes Sema 3A staining. In the two week regenerate cord, the staining pattern observed in the grey matter cells of the intact cord is still present; in addition, staining in the nuclear regions of grey matter cells was present, and expression in the leptomeninges was observed (figure 3.22). Lastly, in the approximately four week regenerate, nuclear localization within grey matter neurons was absent, respective cytoplasmic and perinuclear localization were downregulated, and meningeal localization was also downregulated (figure 3.23).

With regard to Msi-1, label was observed in the cytoplasm, nuclear, and perinuclear regions of grey matter and ependymal cells in lesion tissue (figure 3.25) For GFAP, an intact cord exhibited significant staining within ependymal cell radial processes and endfeet (figure 3.26); the meninges was demonstrated to be GFAP (-). In contrast, respective expression was downregulated in a 14 day regenerate, indicating that the injury reactive ependymal cells were retracting their endfeet and breaking down GFAP, which is an initial step in losing apical/basal polarity. Finally, in mesenchymal ependymal outgrowth, GFAP is expressed only in a few residual islands of mesenchymal cells. Furthermore, these results confirm that Sema 3A, Msi-1, and GFAP are suitable markers for meningeal pia mater and reactive ependymal cells, respectively, which will aid in elucidating the differential expression of retinoids in those cells when used in combination with RALDH2 staining in future studies. A summary of Sema 3A expression is provided in figure 3.24.

3.7 Supporting data: Whole mount ECM staining and antibody labeling using α-chondrotin-4 and -6 sulfate proteoglycan, α-CRABP2, and α-RALDH 2

In order to examine the ECM composition of the regenerating cord, combined alcian blue/metanil yellow whole mount stain was performed on a regenerating cord cord to analyze the presence of proteoglycan and collagen, respectively (courtesy of Sarah Scott, Chernoff Lab student). ECM distribution in the meninges presents and addition property of the control and reactive meningeal layers useful in evaluating the reactive state. Results indicate that in the two week regenerate cord, the meninges contain a large quantity of collagen throughout the meninges as well as a significant deposit of proteoglycan in and several millimeters adjacent to the lesion site (figures 3.28 and 3.29), supporting the fact that when the meninges and ependymal cells undergo EMT to remodel the cord, proteoglycans (i.e.-CSPGs) are indeed present despite an inhibitory role in injured mammalian cord [1, 6]. Both the stump and outgrowth regions of the cord meninges produce collagen, but the proteoglycan is concentrated in the outgrowth zone (figure 3.27).

For comparison to the whole mount ECM stained samples, whole mount stained meninges were labeled with CRABP 2 (figure 3.30) and RALDH 2 (figure 3.31) to characterize meningeal expression: the outermost layers of the dura appear to be missing, but the cellular layers of the meninges are present plus arachnoid and pia. The arachnoid is the most visible layer in these preparations. The meninges significantly expressed CRABP2 and RALDH2, which corroborates with the respective antibody labeling employed on the paraffin sections. Numerous melanocytes, which are characteristic of the arachnoid, were present where these retinoids were being expressed (figures 3.30 and 3.31), suggesting that CRABP2 and RALDH2 are being expressed in the middle meningeal layers. In contrast, although the thin layer superficial to the apparent arachnoid containing the melanocytes was highly cellular, it was essentially devoid of retinoid expression. Furthermore, additional whole mount

stainings performed with these antibodies will need to be performed in order to further elucidate the differential retinoid expression in the meninges.

Finally, axolotl tissue sections were labeled with chondroitin sulfate -4 and -6 proteoglycan antibody via HRP in order to confirm the original Developmental Studies Hybridoma Bank results. Expression was prominent in neurons of the dorsal aspect as well as the meninges. Whole regenerating cord with meninges was then HRP-stained with this antibody, further confirming the results obtained from the peeled cord whole mounts stained with alcian blue and metanil yellow (figure 3.32): specifically, chondroitin sulfate proteoglycans are expressed in the meninges of the regenerating axolotl tissue. The combination of the sections and the whole mount staining studies show that reactive meninges are in the lesion site and that the reaction is propagated cranial and caudal from the lesion site in the reactive stump.

3.8 Quantitation of PCNA expression in adult intact and two week regenerate ependymal zone of cord sections

In order to quantify one aspect of ependymal cell behavior within non-reactive (control) as well as injury reactive ependymal cells, respective tissue sections were labeled with an α-PCNA antibody (cyclin antibody targeting the nuclei of cells that are actively transiting the cell cycle) in order to identify ependymal cells that are mitotically active (figure 3.33). The mitotic index (MI) was then determined utilizing two sets of data for both intact and two week regenerate cord sections (table 3.2). The MI is defined as the ratio of cells binding DAPI (all cell nuclei) to those expressing PCNA. In the intact cord, the average number of cells expressing DAPI and PCNA were 53 ± 2 and 39.5 ± 1.5, respectively, resulting in an average MI of 74.5%. In the two week regenerate (cells comprising the outgrowth), the average number of cells expressing DAPI and PCNA were 120 ± 4 and 94 ± 4, respectively, resulting in an average MI of 78.3 ± 6%.

Moreover, the mitotic indices of the intact cord compared to the regenerate cord are not significantly different from each other, indicating that the respective proliferative activity of ependymal cells during the injury response does not drastically increase. This is consistent with the studies that show the continuous growth of the Urodele spinal cord throughout life [6].

CHAPTER 4: RESULTS AND DISCUSSION-MANIPULATION OF THE CELL CULTURE ENVIRONMENT OF AXOLOTL SPINAL CORD TISSUE EXPLANTS TO STUDY THE ROLE OF RETINOIDS *IN VITRO*

4.1 Confirmation of presence of mesenchymal and epithelial cells and labeling of tissue cultures with α-RALDH 2 and α-CRABP 2 to confirm respective expression in the tissue culture model system

When approximately two week regenerate ependymal and meningeal tissue explants were maintained as a co-culture, mesenchymal outgrowth was observed to be migrating from the ependymal cell explant, oriented in the direction of the meningeal explant (figure 4.1). In addition, the presence of epithelial ependymal cells was confirmed near the meningeal tissue. To demonstrate mesenchymal and epithelial organization in the outgrowth, the fixed cultures were treated with rhodamine-phalloidin to label the actin cytoskeleton. Epithelial ependymal cells displayed tight packing (similar to the appearance of a honeycomb) as well as circumferential sub-apical staining, associated with respective actin attachment to belt desmosomes; mesenchymal cells were elongated and possessed non-circumferential actin bundles (figure 4.2). The initial outgrowth is mesenchymal and the leading edge of outgrowth remains mesenchymal. With time of exposure to the meninges, epithelial regions of ependymal cells appear, typically by two weeks of culture. If this is due to retinoid production, then retinoid biosynthesis components must be maintained in the reactive meninges in culture in the chemically defined culture environment. RALDH2 and CRABP2 production were chosen as the markers of interest. Step one was to verify the

presence of retinoids in regenerating spinal cord explants, consisting of primarily meningeal tissue. While it is possible to clean ependymal outgrowth of clinging meninges completely, it is not possible to remove all of the ependymal cells from reactive meninges due to infiltration of the ependymal into the meningeal ECM. RALDH2 production was chosen as the marker of interest. Cultures consist of ependymal explants with predominantly meningeal explants adjacent or meningeal explants with clinging ependymal cells. When labeled with α-RALDH2, significant expression was present on the meningeal region of the explants, apparently on the surface. The ependymal mesenchymal outgrowth from the explants showed perinuclear RALDH2 staining (figure 4.3). α-CRABP 2-labeled co-cultures composed of ependymal and meningeal tissue explants both exhibited expression of this protein (figure 4.4). These results are consistent with the previously presented *in vivo* immunohistochemical data that demonstrates that RALDH 2 and CRABP2 are present in the reactive meninges and validate the use of this tissue culture system.

To correlate the identity of the meningeal layer labeling in these experiments with the observations made in other species, meningeal explants were labeled with Rhodamine-Phalloidin: the F-actin pattern observed is similar to that observed via SEM in the arachnoid layer of the adult intact cord (figure 4.5; SEM courtesy of Deborah Sarria, Chernoff Lab), strongly resembling the arachnoid border cells in humans and the arachnoid layer in newts [7, 61]. Furthermore, the ECM staining of this same layer also produces results consistent with the identification as arachnoid, as this layer is both highly cellular and produces abundant fibrillary collagen (figures 3.23, 3.26)[61].

4.2 Quantitation of PCNA expression in day 7 ependymal and ependymal/meningeal tissue explants

In order to further examine the effects of reactive meninges on the ependymal outgrowth *in vitro*, reactive pure ependymal cultures and ependymal/meningeal co-cultures were labeled with an α-PCNA antibody (figures 3.33 and 4.6). The MI was calculated from the average number of PCNA-labeled cells. Table 4.1 shows results utlilizing three sets of corresponding data for the pure ependymal tissue cultures and two sets of data for the ependymal/meningeal tissue cultures. In the pure ependymal cell culture, the average number of cells expressing DAPI and PCNA were 48 ± 8 and 24 ± 6, respectively, resulting in an average MI of 49 ± 4%. Prior Chernoff lab studies in which cultures were labeled with 3 [H]-thymidine have shown that pure ependymal explant cultures show an MI of 50-75% (depending on the length of labeling), consistent with the present study [65]. In the ependymal/meningeal tissue culture, the average number of cells expressing DAPI and PCNA were 88 ± 8 and 36 ± 4, respectively, resulting in an average MI of 42 ± 9%. Moreover, like the tissue sections (table 3.4), the mitotic indices of the pure ependymal tissue culture compared to the ependymal/meningeal tissue culture are not significantly different from each other, indicating that the respective proliferative activity of ependymal cells during the injury response does not drastically increase. However, it is interesting to note that microscopic examination of the ependymal/meningeal explants shows and unexpected proximity to the cultured meninges. The leading mesenchymal outgrowth shows a high level of mitotic cells, but the epithelializing zone close to the meninges is non-mitotic as viewed by PCNA labeling (figure 4.7). It is not yet clear whether this is due directly or indirectly to growth and trophic factor production from the meninges, an ECM effect, or cell-contact mediated process.

CHAPTER 5. CONCLUSIONS

Furthermore, the overall conclusions made from the data obtained during this project thus far include:

1) The axolotl meninges is actively producing components of the RA metabolic pathway in intact and regenerating spinal cord.
2) The meningeal layer that shows the greatest retinoid activity is the middle layer, in which ECM content, actin cytoskeleton distribution, and SEM suggest is the arachnoid.
3) The ependymal cells of the adult axolotl cord appear to be inactive in terms of producing retinoids in the intact cord, while the gray matter neurons are active.
4) After injury, there are retinoid pathway positive cells in the lesion site.
5) After injury, the ependymal cells of the stump regions cranial and caudal to the lesion site are retinoid pathway active.
6) Cell proliferation is high in intact ependymal cell population as well as in regenerating cord, which is not unexpected for an animal showing indeterminate (continued) growth. The pattern of proliferation can be modified by some aspect of meningeal contact (as seen in the co-culture experiments), which is associated with some aspect of contact with the reactive meninges.

Further ventures for this project include: completing retinoid pathway staining on mesenchymal outgrowth; using tissue specific markers as well as PCR to confirm expression of RARβ and RXRγ nuclear receptors; perform co-culture experiments using reactive meninges and ependymal cells from lesioned tissue in order to observe their

interaction in the presence of retinoid inhibitors to ultimately determine if retinoids (rather than thrombin or another factor) are specifically facilitating the re-epithelialization of the reactive ependymal cells; perform double-labeling experiments on tissue sections utilizing retinoid and NeuN (neuronal biomarker marker) antibodies to better characterize neuronal retinoid expression; execute osteoclast inhibitor studies in order to further elucidate the effect of retinoids on the reactive meninges; and finally, apply the aforementioned methods on GFP transgenic mice in order to target retinoid expression in the mammal. Overall, the data acquired from this thesis project will aid in the downstream development of translational applications in mammalian spinal cord injuries: elucidation of the retinoic acid pathway as well as other pathways involved in Axolotl spinal cord regeneration can be subsequently performed on identical and/or analogous pathways in the mammal so that respective recoveries will hopefully generate more effective and successful outcomes.

REFERENCES

REFERENCES

1. Diaz Quiroz, J.F., Tsai, E., Coyle, M., Sehm, T., Echeverri, K., Precise Control of miR125b is Required to Create a Regeneration-Permissive Environment After Spinal Cord Injury. Dis Model Mech, 2014. 7(6): p. 601-611.
2. Martini, F.A., Nath, J.L., Fundamentals of Anatomy and Physiology. 2009, Prentice Hall.
3. Bell, R.S., et al., Military Traumatic Brain and Spinal Column Injury: A 5-Year Study of the Impact Blast and Other Military Grade Weaponry on the Central Nervous System. Journal of Trauma and Acute Care Surgery, 2009. 66(4): p. S104-S111
4. Zeilig, G., et al., Civilian spinal cord injuries due to terror explosions. Spinal Cord, 2010. 48(11): p. 814-8.
5. Burnside, E.R.a.B., E.J., Review: Manipulating the extracellular matrix and its role in brain and spinal cord plasticity and repair. Neuropathology and Applied Neurobiology, 2014. 40: p. 26-59.
6. Chernoff, E.A.G., Stocum. D.L., Nye, H.L.D., and Cameron, J.A., Urodele Spinal Cord Regeneration and Related Processes. Developmental Dynamics, 2003. 226: p. 295-307.
7. Zukor, K.A., Kent, D.T., Odelberg, S.J., Meningeal Cells and Glia Establish a Permissive Environment for Axon Regeneration After Spinal Cord Injury in Newts. Neural Development, 2011. 6(1): p. 1-22.
8. Mchedlishvili, L., Mazurov, V., Grassme, K.S., Goehler, K., Robl, B., Tazaki, A., Roensch, K., Tanaka, E.M., Reconstitiution of the Central and Peripheral Nervous System During Salamander Tail Regeneration. Proc. Nat. Acad. Sci., 2011. 109(34): p. E2258-E2266.
9. Egar, M., Singer, M., The Role of Ependyma in Spinal Cord Regrowth, in Mechanisims of Growth Control, R.O. Becker, Editor. 1981, Charles Thomas: Springfield, Il. p. 93-106.
10. Shimada, J.-I., Taniguchi, J., Mori, M., Sato, Y., Takuwa, H., Ito, H., Kuwabara, S., Retinol Palmitate Prevents Ischemia-Induced Cell Changes in Hippocampal Neurons Through the Notch1 Signaling Pathway in Mice. Experimental Neurology, 2013. 247: p. 182-187.
11. Wolf, G., Tissue-Specific Increases In Endogenous All-Trans Retinoic Acid: Possible Contributing Factor In Ethanol Toxicity. Nutrition Reviews, 2010. 68(11): p. 689-692.

12. Zhang, J., Smith, D., Yamamoto, M., Ma, L., McCaffery, P., The Meninges Is a Source of Retinoic Acid for the Late-Developing Hindbrain. The Journal of Neuroscience, 2003. 23(20): p. 7610-7620.
13. Maden, M., Hind, M., Retinoic acid: a Regeneration-Inducing Molecule. Developmental Dynamics, 2003. 226: p. 237-244.
14. Bushue, N., Yu-Jui, Y.W., Retinoid Pathway and Cancer Therapeutics. Adv Drug Deliv Rev, 2010. 62(13): p. 1285-1298.
15. Carter, C., Clark, A., Spencer, G., Carlone, R., Cloning and Expression of a Retinoic Acid Receptor β2 Subtype From the Adult Newt: Evidence for an Early Role in Tail and Caudal Spinal Cord Regeneration. Developmental Dynamics, 2011. 240: p. 2613-2625.
16. Theodosiou, M., Monaghan, J.R., Spencer, M.L., Voss, S.R., Noonan, D.J., Isolation And Characterization of Axolotl NPDC-1 And Its Effects on Retinoic Acid Receptor Signaling. Comp Biochem Physiol Mol Biol, 2007. 147(2): p. 260-270.
17. Agudo, M., Yip, P., Davies, M., Bradbury, E., Doherty, P., McMahon, S., Maden, M., Corcoran, J.P.T, A Retinoic Acid receptor β Agonist (CD2019) Overcomes Inhibition of Axonal Outgrowth via Phosphoinositide 3-Kinase Signaling in the Injured Adult Spinal Cord. Neurobiol Dis, 2010. 37(1): p. 147-155.
18. van Neerven, S., Mey, J., Joosten, E.A., Steinbusch, H.W., van Kleef, M., Marcus, M.A.E., Deumens, R., Systemic But Not Local Administration of Retinoic Acid Reduces Early Transcript Levels of Pro-Inflammatory Cytokines After Experimental Spinal Cord Injury. Neuroscience Letters, 2010. 485: p. 21-25.
19. Maden, M., Holder., N., The Involvement of Retinoic Acid in the Development of the Vertebrate Central Nervous System. Developmental Supplement 2, 1991: p. 87-94.
20. Maden, M., The Effect of Vitamin A on the Regenerating Axolotl Limb. J.Embryol. exp. Morph., 1983. 77: p. 273-295.
21. McCormick, A.M., Shubeita, H.E., Stocum, D.L., Cellular Retinoic Acid Binding Protein: Detection and Quantitation in Regenerating Axolotl Limbs. The Journal of Experimental Zoology, 1988. 245: p. 270-276.
22. Monkemeyer, J., Ludolph, D.C., Cameron, J.A., Stocum, D.L., Retinoic Acid-Induced Change in Anteroposterior Positional Identity in Regenerating Axolotl Limbs Is Dose-Dependent. Developmental Dynamics, 1992. 193: p. 286-294.
23. Scadding, S.R., Maden, M., Retinoic Acid Gradients during Limb Regeneration. Developmental Biology, 1994. 162: p. 608-617.
24. Johnson, K.J., Scadding, S.R., Effects of Tunicamycin on Retinoic Acid Induced Respecification of Positional Values in Regenerating Limbs of the Larval Axolotl, *Ambystoma mexicanum*. Developmental Dynamics, 1992. 193: p. 185-192.
25. Maden, M., Holder., N., Retinoic Acid and Development of the Central Nervous System. Bioessays, 1992. 14(7): p. 431-438.
26. Ludolph, D.C., Cameron, J.A., Stocum, D.L., The Effect of Retinoic Acid on Positional Memory in the Dorsoventral Axis of Regenerating Axolotl Limbs. Developmental Biology, 1990. 140: p. 41-52.

27. Giguère, V., Ong, E.S., Evans, R.M., Tabin, C.J., Spatial and Temporal Expression of the Retinoic Acid Receptor in the Regenerating Amphibian Limb. Nature, 1989. 337: p. 566-569.
28. Kim, W.S., Stocum, D.L., Retinoic Acid Modifies Positional Memory in the Anteroposterior Axis of Regenerating Axolotl Limbs. Developmental Biology, 1986. 114: p. 170-179.
29. del Rincón, S.V., Scadding, S.R., Retinoid Antagonists Inhibit Normal Patterning During Limb Regeneration in the Axolotl, *Ambystoma mexicanum*. Journal of Experimental Zoology, 2002. 292: p. 435-443.
30. Maden, M., Retinoids as Endogenous Components of the Regenerating Limb and Tail. Wound Repair and Regeneration, 1998. 6: p. 358-365.
31. Monaghan, J.R., Maden, M., Visualization of Retinoic Acid Signaling in Transgenic Axolotls During Limb Development and Regeneration. Developmental Biology, 2012. 368: p. 63-75.
32. Chernoff, E.A.G., Henry, L.C., Spotts, T., An Ependymal Cell Culture System for the Study of Spinal Cord Regeneration. Wound Repair and Regeneration, 1998. 6: p. 403-412.
33. Hsieh, H.-L., Tung, W-H., Wu, C-Y., Wang, H-H., Lin, C-C., Wang, T-S., Yang, C-M., Thrombin Induces EGF Receptor Expression and Cell Proliferation via a PKC(δ)/c-Src-Dependent Pathway in Vascular Smooth Muscle Cells. Arterioscler Thromb Vasc Biol., 2009. 29: p. 1594-1601.
34. Harlan, J.M., Thompson, P.J., Ross, R.R., Bowen-Pope, D.F., Alpha-thrombin induces release of platelet-derived growth factor-like molecule(s) by cultured human endothelial cells. J. Cell Biol, 1986. 103(3): p. 1129-1133.
35. McDonough, A., Martínez-Cerdeño, V., Endogenous Proliferation after Spinal Cord Injury in Animal Models. Stem Cells International, 2012. 2012: p. 1-16.
36. Hugnot, J.P., Franzen, R., The Spinal Cord Ependymal Region: A Stem Cell Niche in the Caudal Central Nervous System. Frontiers in Bioscience, 2011. 16: p. 1044-1059.
37. Lacroix, S., Hamilton, L.K., Vaugeois, A., Beaudoin, S., Breault-Dugas, C., Pineau, I., Lévesque, S.A., Grégoire, C-A., Fernandes, K.J.L., Central Canal Ependymal Cells Proliferate Extensively in Response to Traumatic Spinal Cord Injury but not Demyelinating Lesions. PLoS ONE, 2014. 9(1): p. 1-11.
38. Chernoff, E.A.G., Munck, C.M., Mendelsohn, L.G., Egar, M.W., Primary Culture of Axolotl Spinal Cord Ependymal Cells. Tissue and Cell, 1990. 22(5): p. 601-613.
39. Fletcher, T.F. Veterinary Neurohistology. CNS: white and Gray matter 2007 June 2011 [cited 2014 31 July 2014].
40. Judson Herrick, C., The Membranous Parts of the Brain, Meninges, and their Blood Vessels in Amblystoma. Journal of Comparative Neurology, 1935. 61(2): p. 297-346.
41. Zammit, P.S., Clarke, J.D.W., Golding, J.P., Goodbrand, I.A., Tonge, D.A., Macrophage Response During Axonal Regeneration in the Axolotl Central and Peripheral Nervous System. Neuroscience, 1993. 54(3): p. 781-789.

42. Grimpe, B., Pressman, Y., Bunge, M.B., Silver, J., The role of proteoglycans in Schwann cell/astrocyte interactions and in regeneration failure at PNS/CNS interfaces. Molecular and Cellular Neuroscience, 2005. 28(1): p. 18-29.
43. O'Hara, C.M., Egar, M.W., Chernoff, E.A.G, Reorganization of the Ependyma During Axolotl Spinal Cord Regeneration: Changes in Intermediate Filament and Fibronectin Expression. Developmental Dynamics, 1992. 193: p. 103-115.
44. Silver, J., Miller, J.H., Regeneration beyond the glial scar. Nat Rev Neurosci, 2004. 5(2): p. 146-156.
45. Klapka, N., Müller, H.W., Collagen Matrix in Spinal Cord Injury. Journal of Neurotrauma, 2006. 23(3/4): p. 422-435.
46. Avram, S., Shaposhnikov, S., Buiu, C., Mernea, M., Chondroitin Sulfate Proteoglycans: Strucutre-Function Relationship with Implication in Neural Development and Brain Disorders. Biomed Research International, 2014: p. 1-11.
47. Iseki, K., Hagino, S., Nikaido, T., Zhang, Y., Mori, T., Yokoya, S., Hozumi, Y., Goto, K, Wanaka, A., Tase, C., Gliosis-specific transcription factor OASIS coincides with proteoglycan core protein genes in the glial scar and inhibits neurite outgrowth. Biomed Res, 2012. 33(6): p. 345-353.
48. Clugston, R.D., Blaner, W.S., Vitamin A (Retinoid) Metabolism and Actions: What We Know and What We Need to Know About Amphibians. Zoo Biology, 2014. 9999: p. 1-9.
49. Hunter, K., Maden, M., Summerbell, D., Eriksson, U., Holder., N., Retinoic Acid Stimulates Neurite Outgrowth in the Amphibian Spinal Cord. Proc. Nat. Acad. Sci., 1991. 88: p. 3666-3670.
50. Mey, J., New Therapeutic Target for CNS Injury? The Role of Retinoic Acid Signaling after Nerve Lesions. Journal of Neurobiology, 2006. 66: p. 757-779.
51. Tanaka, M., Tamura, K., and Ide, H., Citral, an Inhibitor of Retinoic Acid Synthesis, Modifies Chick Limb Development. Developmental Biology, 1996. 175: p. 239-247.
52. Kurokawa, R., Söderström, M., Hörlein, A., Halachmi, S., Brown, M., Rosenfeld, M.G., Glass, C.K., Polarity-Specific Activities of Retinoic Acid Receptors Determined by a Co-Repressor. Nature, 1995. 377(5): p. 451-454.
53. Kern, J., Schrage, K., Koopmans, G.C., Joosten, E.A., McCaffery, P., Mey, J., Characterization of Retinaldehyde Dehydrogenase-2 Induction in NG2-Positive Glia After Spinal Cord Contusion Injury. Int. J. Devl Neuroscience, 2007. 25: p. 7-16.
54. Scadding, S.R., Citral, an Inhibitor of Retinoic Acid Synthesis, Modifies Pattern Formation During Limb Regeneration in the Axolotl *Ambystoma mexicanum*. Can. J. Zool., 1999. 77: p. 1835-1837.
55. IHC-P Immunohistochemistry Protocol. 2014 1 November 2014]; Available from: http://www.abcam.com/.
56. Technologies, L. Rhodamine Phalloidin R415 Description. 2015 [cited 2015 8 February 2015]; Available from: https://www.lifetechnologies.com/order/catalog/product/R415.

57. GraphPad Software, I., GraphPad Statistics Guide. 1995-2015.
58. Vector Laboratories, I., Enzyme Immunoassays, Hybridoma Screening, and Western Blots. 2012.
59. Reina, M.A.e.a., The origin of the spinal subdural space: ultrastructure findings. Anesth Analg, 2002. 94: p. 991-995.
60. Reina, M.A.e.a., Ultrastructural findings in human pia mater in relation to subarachnoid anesthesia. Anesth Analg, 2004. 98: p. 1479-1485.
61. Vandenabeele, F., Creemers, J., and Lambrichts, I., Ultrastructure of the human spinal arachnoid mater and dura mater. J. Anat, 1996. 189: p. 417-430.
62. Davis, B.M., Duffy, M.T., Simpson., S.B. Jr., Bulbospinal and Intraspinal Connections in Normal and Regenerated Salamander Spinal Cord. Experimental Neurology, 1989. 103: p. 41-51.
63. Meletis, K., Barnabé-Heider, F., Carlén, M., Evergren, E., Tomilin, N., Shupliakov, O., Frisén, J., Spinal Cord Injury Reveals Multilineage Differentiation of Ependymal Cells. PLoS Biol 2008. 6(7): p. 1-14.
64. Imai, T., Tokunaga, A., Yoshida, T., Hashimoto, M., Mikoshiba, K., Weinmaster, G., Nakafuku, M., Hideyuki Okano, H., The Neural RNA-Binding Protein Musashi1 Translationally Regulates Mammalian numb Gene Expression by Interacting with Its mRNA. Mol. Cell Biol, 2001. 21(12): p. 3888-3900.
65. O'Hara, C.M., Chernoff, E.A.G., Growth factor modulation of injury-reactive ependymal cell proliferation and migration. Tissue and Cell, 1994. 26(4): p. 599-611.

TABLES

Table 2.1 List of antibodies investigated. Names of primary and secondary antibodies utilized are identified along with respective vendor supplier, catalogue number, and working concentrations. *all RARβ antibodies tested failed to work in axolotl tissue. **a goat-anti-mouse IgM should have been utilized

Primary antibody	Primary Antibody vendor and catalogue number	Primary antibody concentration	Secondary antibody	Secondary antibody vendor and catalogue number	Secondary Antibody concentration
Rabbit polyclonal CRABP 2	Abcam Inc. ab74365	1:100	Goat anti-rabbit IgG (H+L) BA-1000	Vector Laboratories	1:200
Rabbit polyclonal CRBP 1	ThermoFisher Scientific PA5-28713	1:200	Goat anti-rabbit IgG (H+L) BA-1000	Vector Laboratories	1:400
Rabbit polyclonal RXRγ	ThermoFisher Scientific PA1-38583	1:100	Goat anti-rabbit IgG (H+L) BA-1000	Vector Laboratories	1:200
Rabbit polyclonal RALDH 2	Abcam Inc. ab96060	1:100	Goat anti-rabbit IgG (H+L) BA-1000	Vector Laboratories	1:200
Rabbit Polyclonal RARβ*	Abcam Inc. ab15515	1:100	Goat anti-rabbit IgG (H+L) BA-1000	Vector Laboratories	1:200
Mouse monoclonal RARβ*	Millipore MABC302	1:25, 1:50	Goat anti-mouse IgG (H+L)**	Vector Laboratories	1:100, 1:200, 1:500
Rabbit polyclonal RARβ*	Acris Antibodies AP15758PU-M	1:100	Goat anti-mouse IgG BA-2020	Vector Laboratories	1:200
Goat polyclonal hMsi-1	R&D Systems AF2628	1:15	Horse anti-goat IgG (H+L) BA-9500 Donkey anti-goat IgG (H+L) Alexa Fluor 594 A-11058	Vector Laboratories Invitrogen	1:200 1:2000
Rabbit polyclonal Sema3A	Abcam Inc. ab 23393	1:40	Goat anti-rabbit IgG BA-1000	Vector Laboratories	1:200
Rabbit polyclonal GFAP	Dako Z0334	1:200	Goat anti-rabbit IgG (H+L) Alexa Fluor 594 A-11037	Invitrogen	1:500

Table 2.2 Axolotl basal media components. Leibovitz L15 was utilized as the primary nutrient source, and supplemented with the listed reagents. Amounts are listed per 50ml of total medium at pH 7.6

Reagent	Amount (ml)
Leibovitz L15 (with L-glutamate)	48.5
Nuclease free water	1.5
Selenium (30 nM)	1.5
Putrescine (100 µM)	0.5
Progesterone (20nM)	1
Insulin (5µg/ml)	1
Transferrin (100 µg/ml)	0.5
EGF (1:500)	0.05
PSF	0.5

Table 2.3 Summary of retinoid cell culture studies *in vitro*. Ependymal/meningeal or pure ependymal tissue explants were subjected to a variety of environmental conditions to observe if ependymal cell behavior correlates with that observed *in vivo*.

Reactive cell type(s)	**Medium + EGF**	**Exogenous Components**	**Purpose**	**Control/Experiment**
Meninges/ ependyma	yes	no	Observe if retinoids are in the meninges and facilitating epithelializaiton	Control
Meninges/ependyma	yes	Labeling with Rhodamine-Phalloidin	Confirm presence of epithelial and mesenchymal cells	Control
Meninges	yes	Antibody labeling with RALDH 2	Confirm if RALDH 2 is upregulated during acute injury	Control
Meninges/ependyma	yes	Antibody labeling with CRABP 2	Confirm expression of CRABP 2 in spinal cord tissue	Control

Table 3.1 Summary of retinoid expression based upon qualitative measurement of global differential spatial and temporal expression patterns.

A) CRBP 1 expression

	Ependyma	Grey Matter	Pia	Arachnoid	Dura
Intact Cord	+	++	+	++	++
2 week regenerate	+++	+++	+++	++	++
5 week regenerate	-	+	-	+	++

B) CRABP 2 expression

	Ependyma	Grey Matter	Pia	Arachnoid	Dura
Intact Cord	+	++	-	+++	+++
2 week regenerate	+++	++	-	+++	+++
5 week regenerate	-	+	-	+++	+++

C) RALDH 2 expression

	Ependyma	Grey Matter	Pia	Arachnoid	Dura
Intact Cord	++	+++	+++	+++	+++
2 week regenerate	+++	+++	+++	+++	+++
5 week regenerate	-	-	+	+	+

*(-) no expression; (+) weak expression; (++) moderate expression; (+++) strong expression.

Table 3.2 Summary of ependymal zone expression of PCNA in intact cord (A) as well as two week regenerate cord tissue section (B). Data sets were obtained and the number of cells expressing DAPI and PCNA in each were each averaged. The MI was subsequently calculated by taking the ratio of the average number of cells expressing PCNA: DAPI (i.e.-using the data in the last row of the table). Each set consisted of 3-4 animals.

A. Intact Adult Axolotl Spinal Cord Ependymoglia

	DAPI	**PCNA**	**MI**
Set 1	51	38	74.5%
Set 2	55	41	74.5%
Set 3	53±2	39.5±1.5	74.5%

B. Adult 2 Week Regenerate Axolotl Spinal Cord (outgrowth end)

	DAPI	**PCNA**	**MI**
Set 1	116	98	84.5%
Set 2	124	90	72.6%
Set 3	120±4	94±4	78.3%±6

*DAPI=DNA stain, all nuclei; PCNA= mitotically active cells;
MI=mitotic index (PCNA/DAPI)
**Data is represented as average ± SEM

Table 4.1 Summary of ependymal zone expression of PCNA in pure ependymal cell (A) as well as ependymal/meningeal tissue explants (B). Data sets were obtained and the number of cells expressing DAPI and PCNA in each were each averaged. The MI was subsequently calculated by taking the ratio of the average number of cells expressing PCNA: DAPI (i.e. using the data in the last row of the table). Each set consisted of 3-4 animals.

A. Pure ependymal tissue explants

	DAPI	**PCNA**	**MI**
Set 1	57	30	53%
Set 2	40	18	45%
Set 3	47	23	49%
Avg.	48±8	24±6	49%±2.3

B. Ependymal/meningeal tissue explants

	DAPI	**PCNA**	**MI**
Set 1	96	32	33%
Set 2	79	40	51%
Avg.	88±8	36±4	42%±9

*DAPI=DNA stain, all nuclei; PCNA= mitotically active cells;
MI=mitotic index (PCNA/DAPI)
**Data is represented as average ± SEM

FIGURES

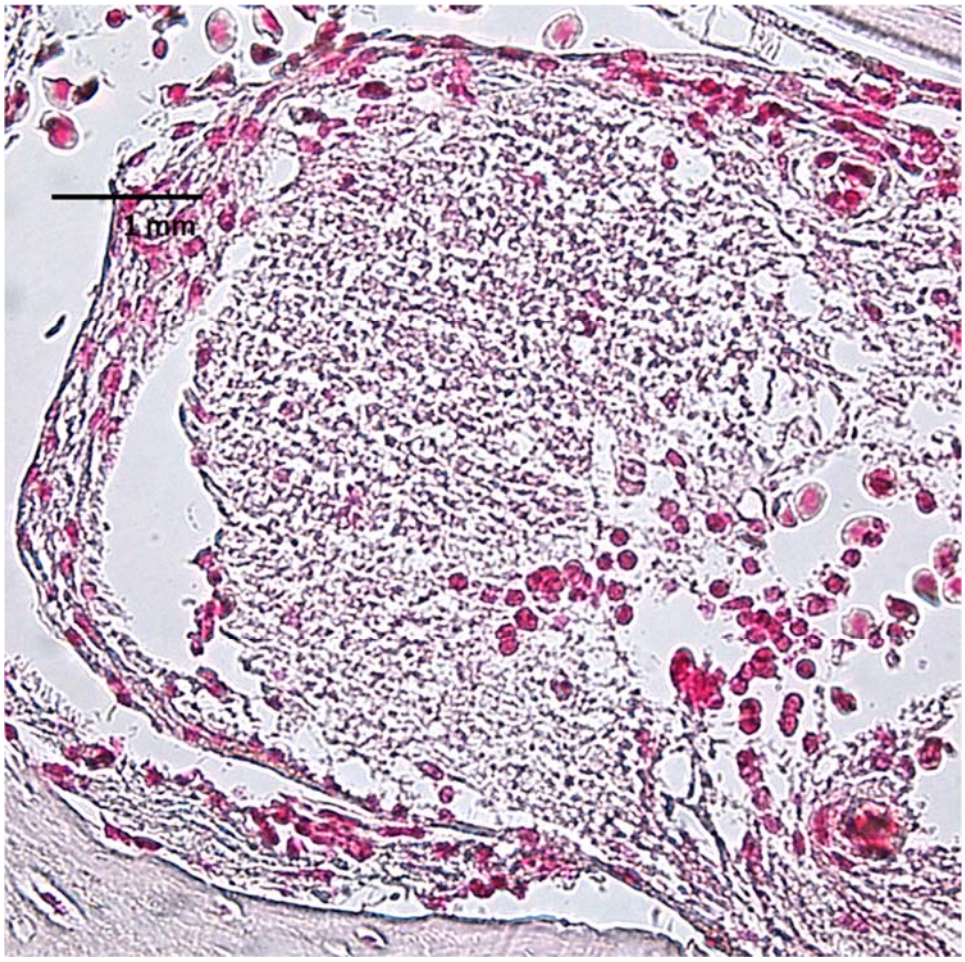

Figure 3.1 Brightfield image of an adult intact cord negative control. No peroxidase label is present when peptide blocking and secondary antibody application are applied. 20x magnification.

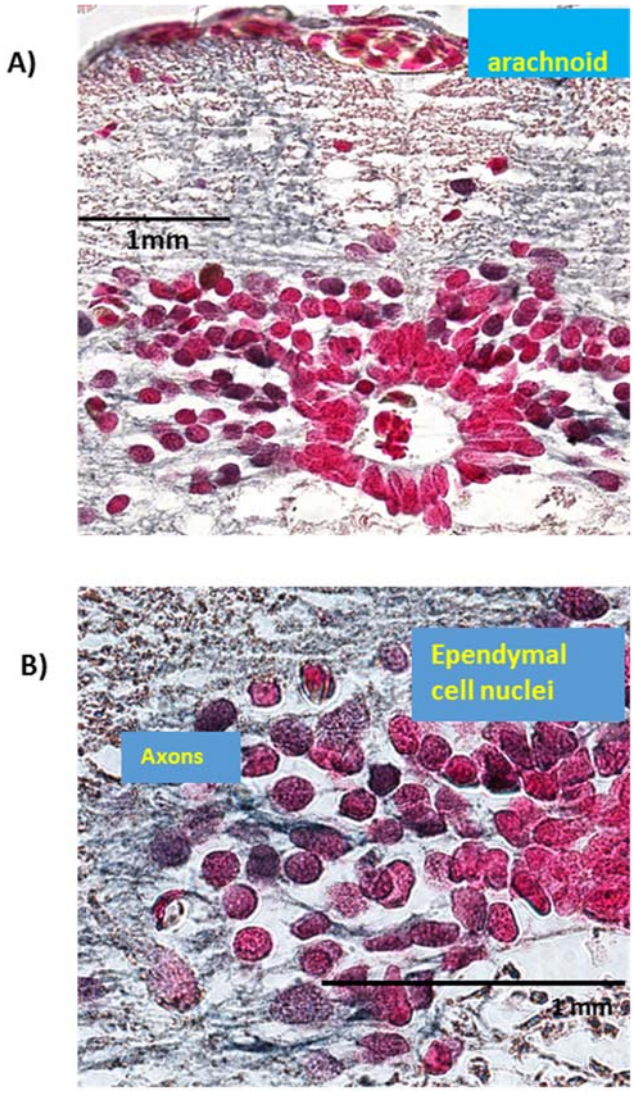

Figure 3.2 Bright field images of an intact cord section labeled with α-CRBP 1 near central canal. Significant axonal/neuronal localization in the grey matter is present. Peroxidase/antibody stain in black; Nuclear fast red stain in red (nuclei). 20x (A) and 40x (B) magnification, respectively.

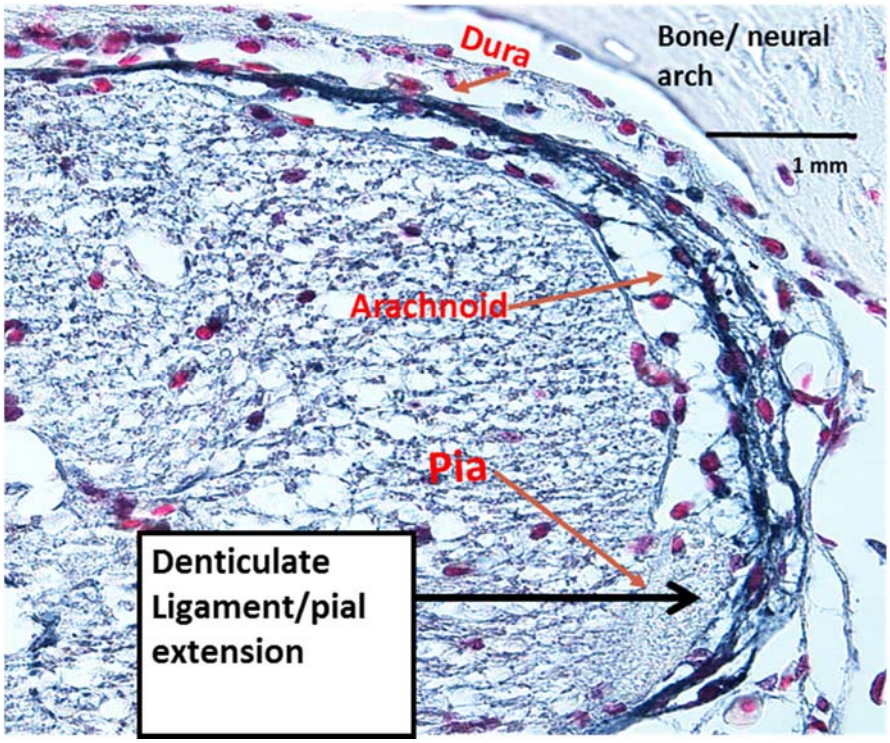

Figure 3.3 Brightfield image of the lateral edge of an intact cord section labeled with α-CRABP 2. Expression is present within the dura/arachnoid. Peroxidase/antibody stain in black; Nuclear fast red stain in red (nuclei). 20x magnification.

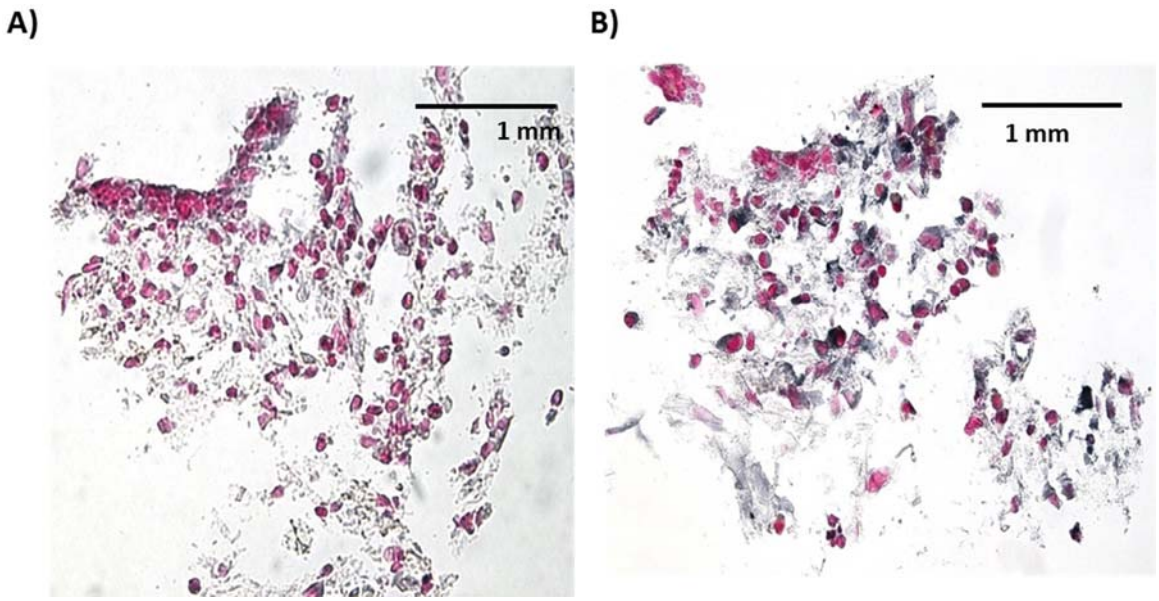

Figure 3.4 Bright field images of two week regenerate cord sections labeled with α-CRBP 1 (A) and α-CRABP 2 (B) near the mesenchymal outgrowth. Peroxidase/antibody stain in black; Nuclear fast red stain in red (nuclei). 20x magnification.

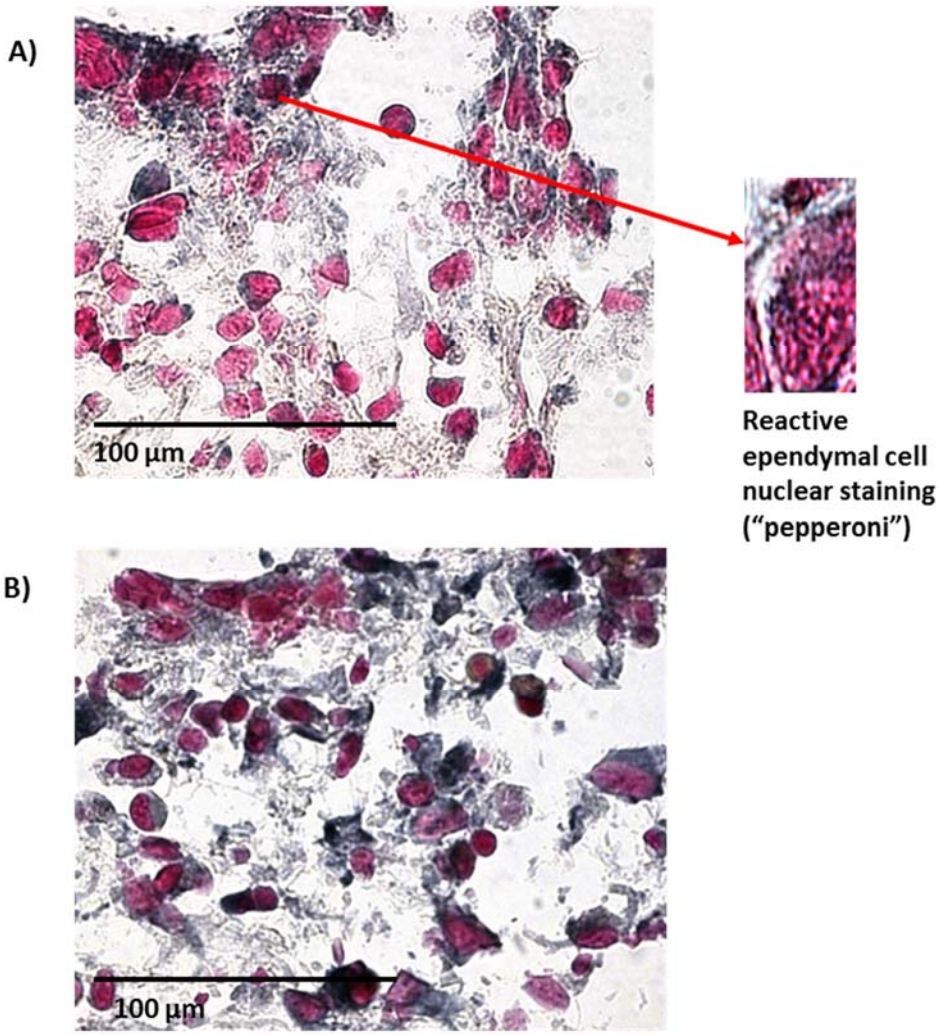

Figure 3.5 Bright field images of two week regenerate cord sections labeled with α-CRBP 1 (A) and α-CRABP 2 (B). Peroxidase/antibody stain in black; Nuclear fast red stain in red (nuclei). 40x magnification.

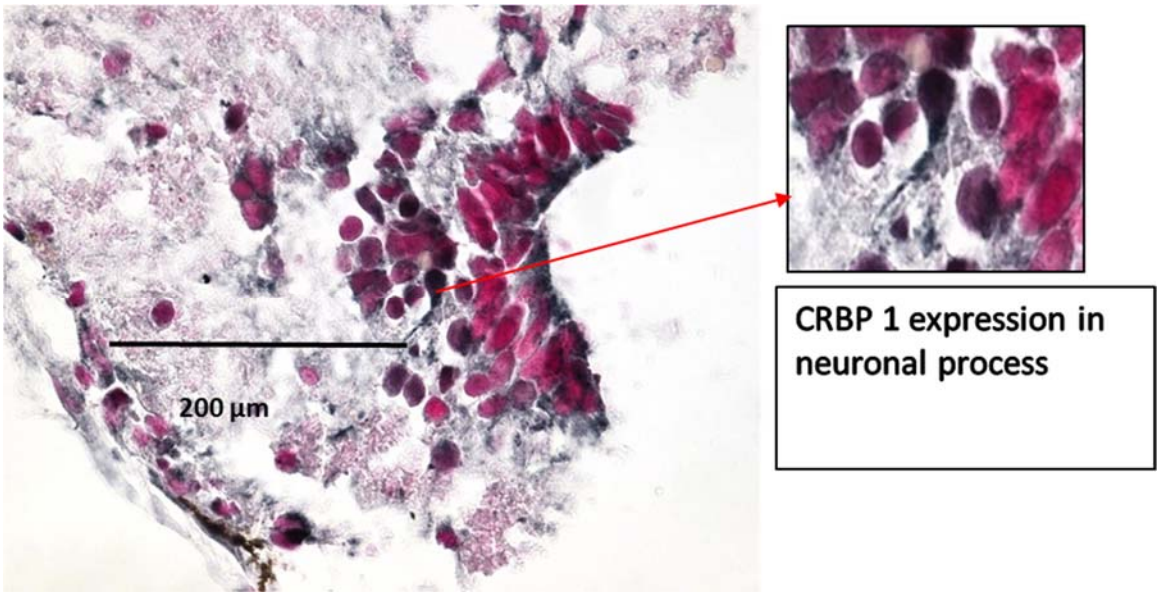

Figure 3.6 Bright field image of a two week regenerate stump cord section labeled with α-CRBP 1. Expression is upregulated in the cell bodies and processes of grey matter neurons as well as in ependyma. Peroxidase/antibody stain in black; Nuclear fast red stain in red (nuclei). 40x magnification.

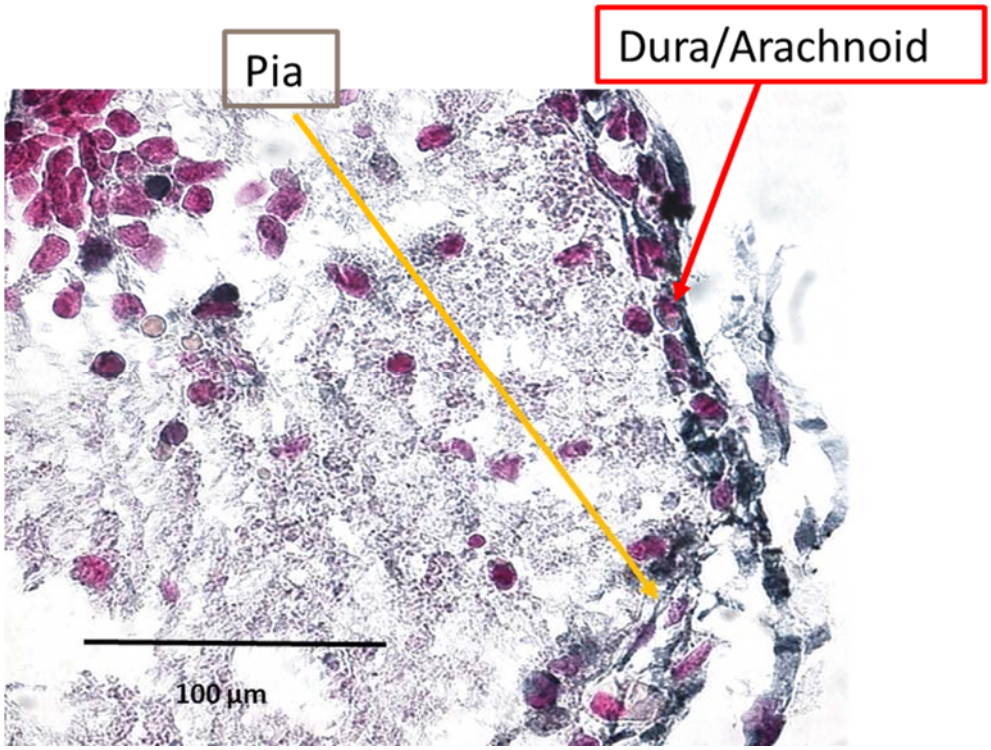

Figure 3.7 Bright field image of a two week regenerate stump cord section labeled with α-CRABP 2. Expression is activated in the pia and some perinuclear accumulation within grey matter cells is also present. Peroxidase/antibody stain in black; Nuclear fast red stain in red (nuclei). 40x magnification.

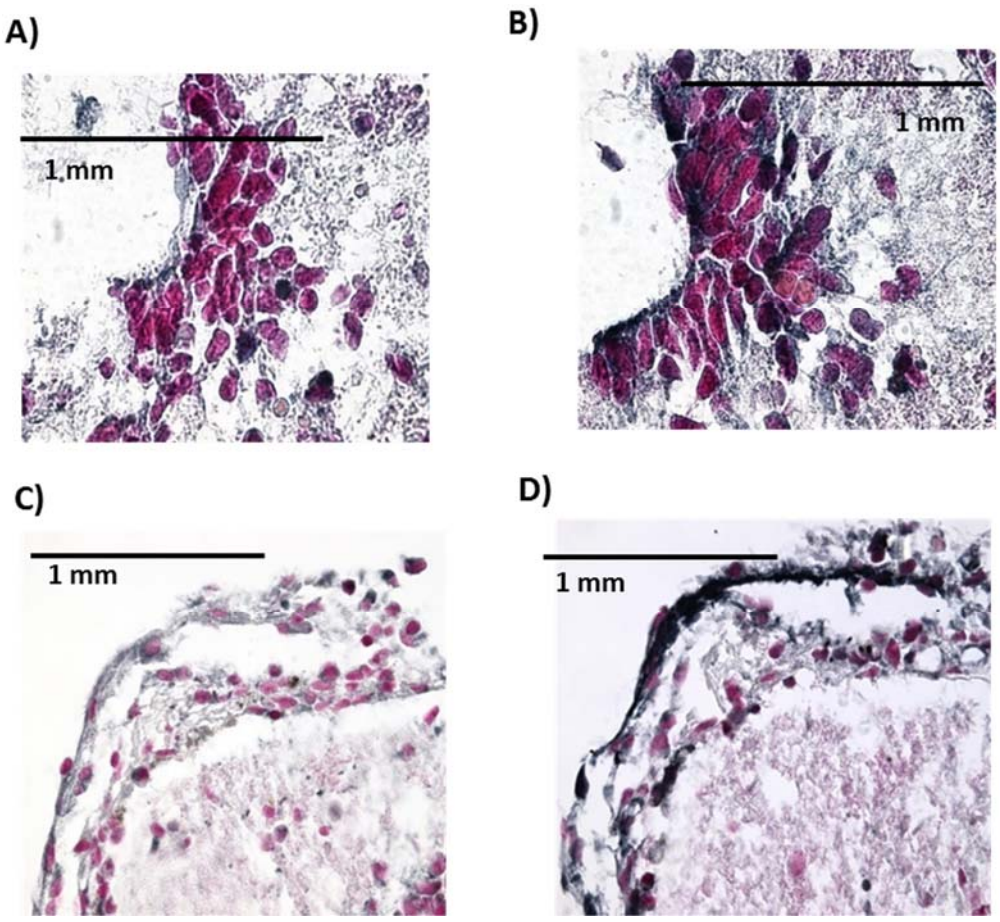

Figure 3.8 Bright field images of two week regenerate stump cord sections labeled with α-CRBP 1 (A and C) and α-CRABP 2 (B and D). Both proteins exhibit cytoplasmic staining within ependymal cells. However, when looking at differential expression within the meninges, CRABP 2 (D) is more heavily expressed compared to CRBP 1 (C). Peroxidase/antibody stain in black; Nuclear fast red stain in red (nuclei). 40x magnification.

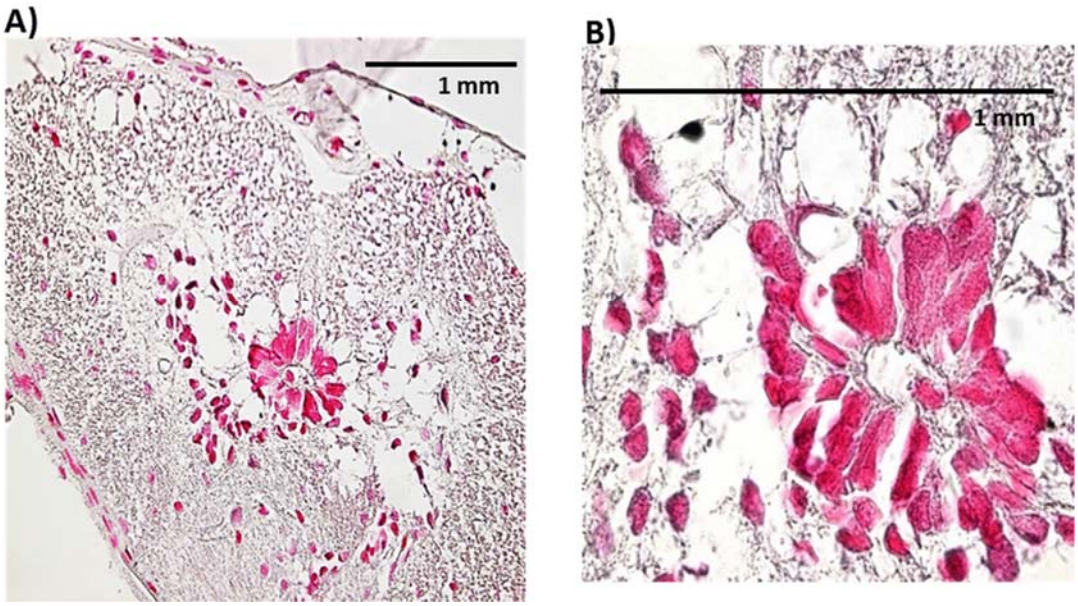

Figure 3.9 Bright field images of a five week regenerate stump cord section labeled with α-CRBP 1. CRBP 1 is weakly expressed in a layer of the meninges (A). The ependyma are negative (B). Peroxidase/antibody stain in black; Nuclear fast red stain in red (nuclei). 20x (A) and 60x (B) magnification, respectively.

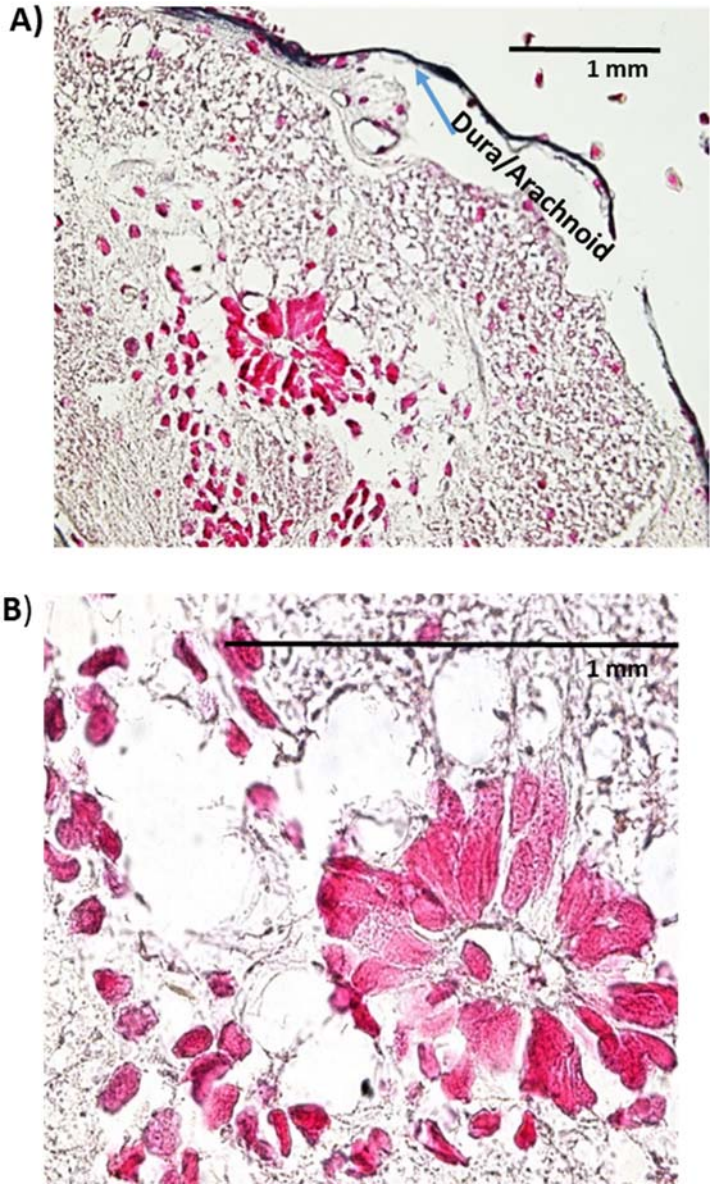

Figure 3.10 Bright field images of a five week regenerate stump cord section labeled with α-CRABP 2. CRABP 2 is significantly expressed in the dura/arachnoid and is negative in the ependyma. Peroxidase/antibody stain in black; Nuclear fast red stain in red (nuclei). 20x (A) and 60x (B) magnification, respectively.

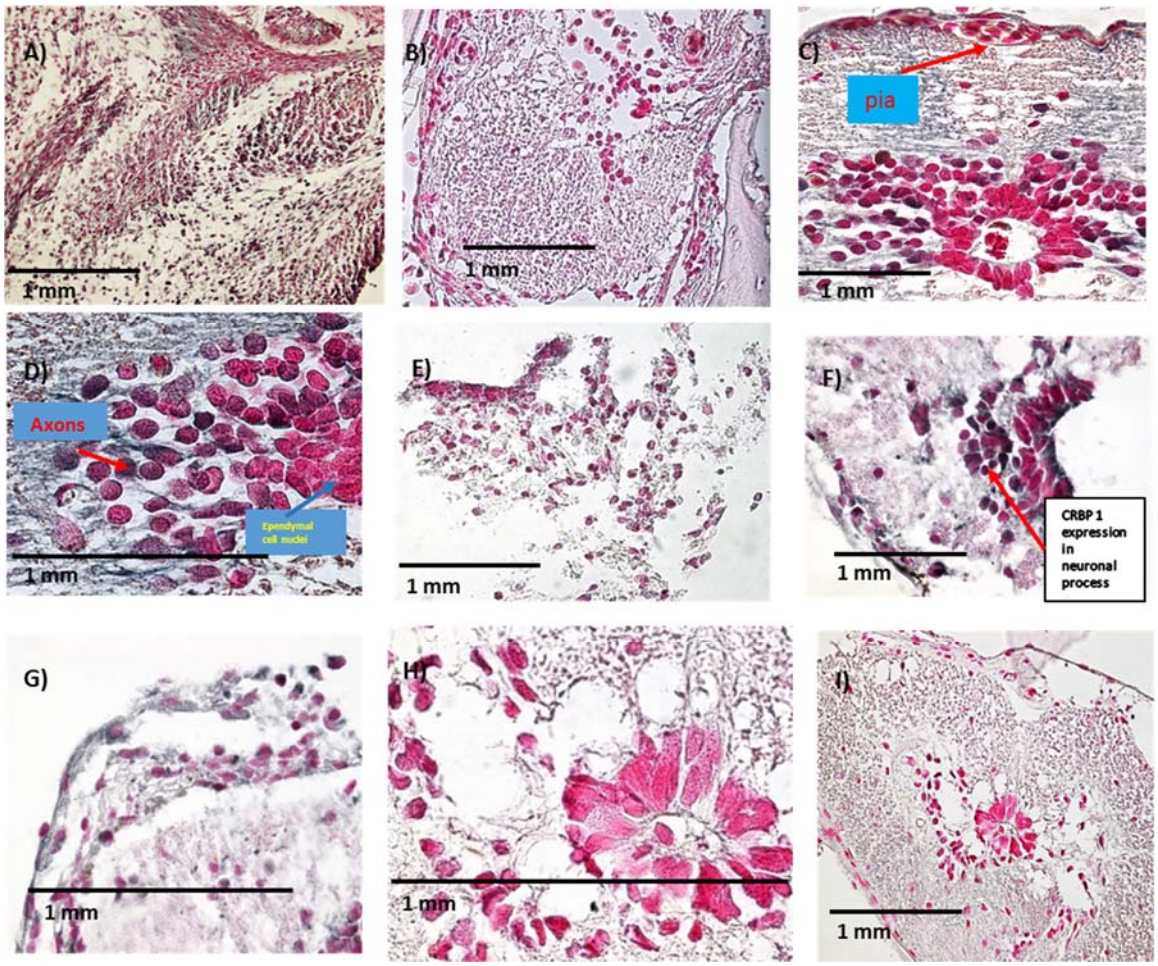

Figure 3.11 Summary of CRBP 1 expression. Mouse embryo positive control (A). Axolotl intact cord negative control (B). Intact cord (C and D). Two week regenerate cord (E). Two week regenerate cord stump (F and G). Five week regenerate (H and I).

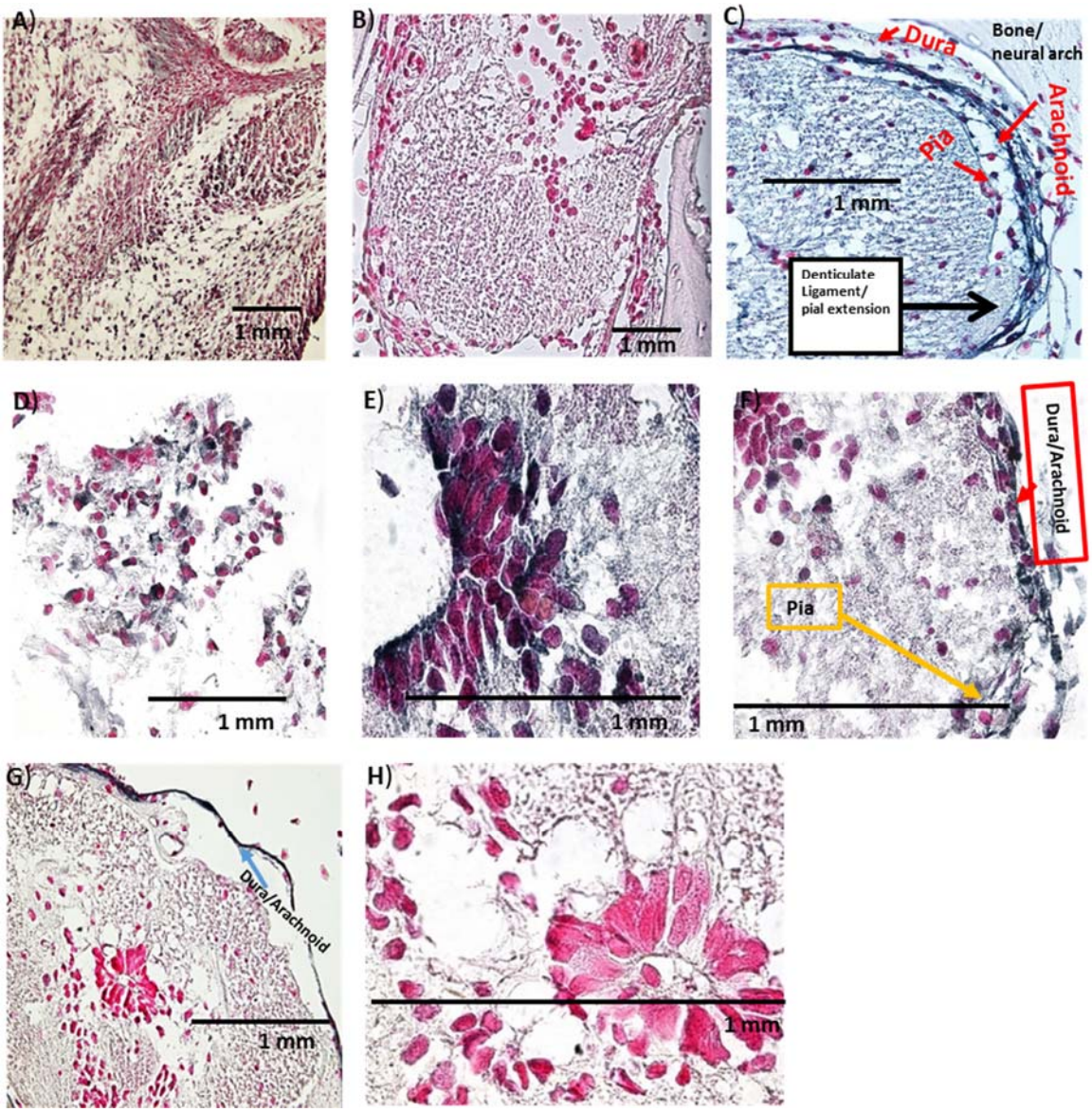

Figure 3.12 Summary of CRABP 2 expression. Mouse embryo positive control (A). Axolotl intact cord negative control (B). Intact cord (C). Two week regenerate cord (D). Two week regenerate cord stump (E and F). Five week regenerate (G and H).

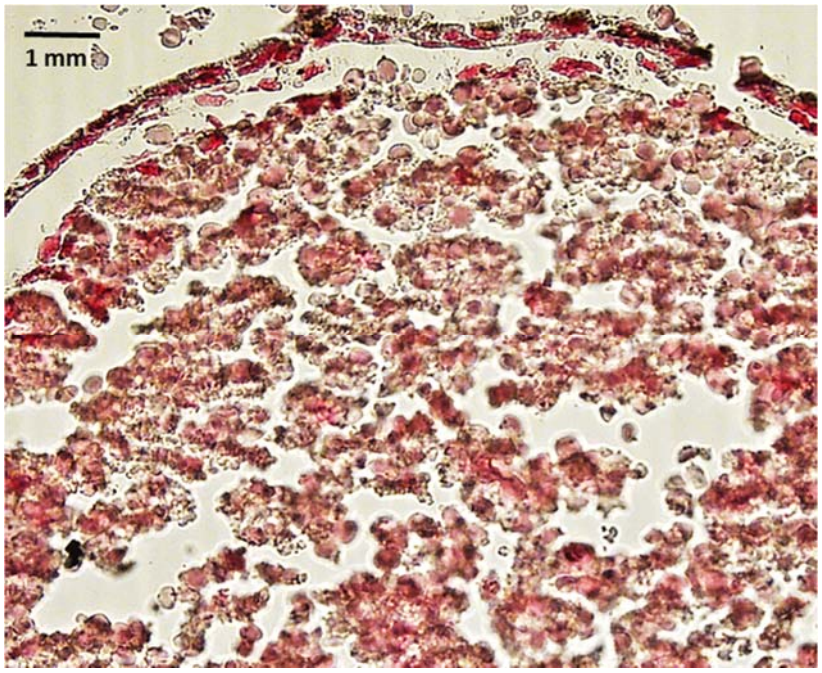

Figure 3.13 Bright field image of an embryonic axolotl spinal cord. RXRγ is not localized within nuclei. 10x magnification.

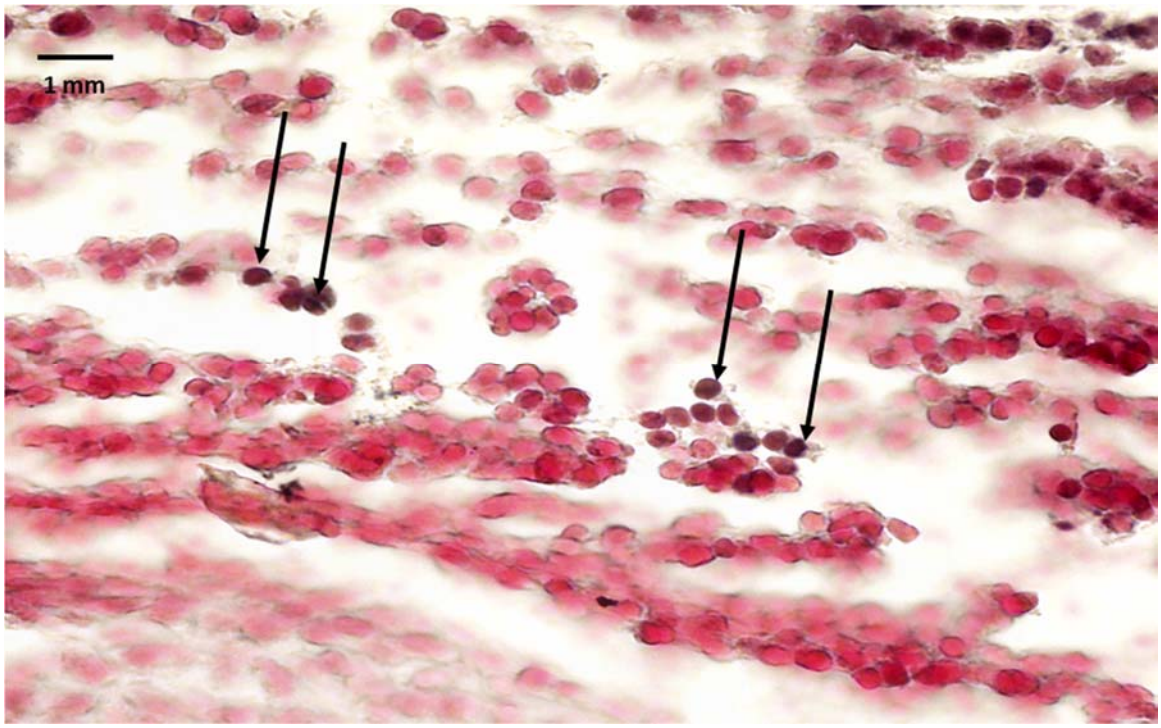

Figure 3.14 Bright field image of a mouse embryo exhibiting some nuclear localization of RXRγ. 10x magnification.

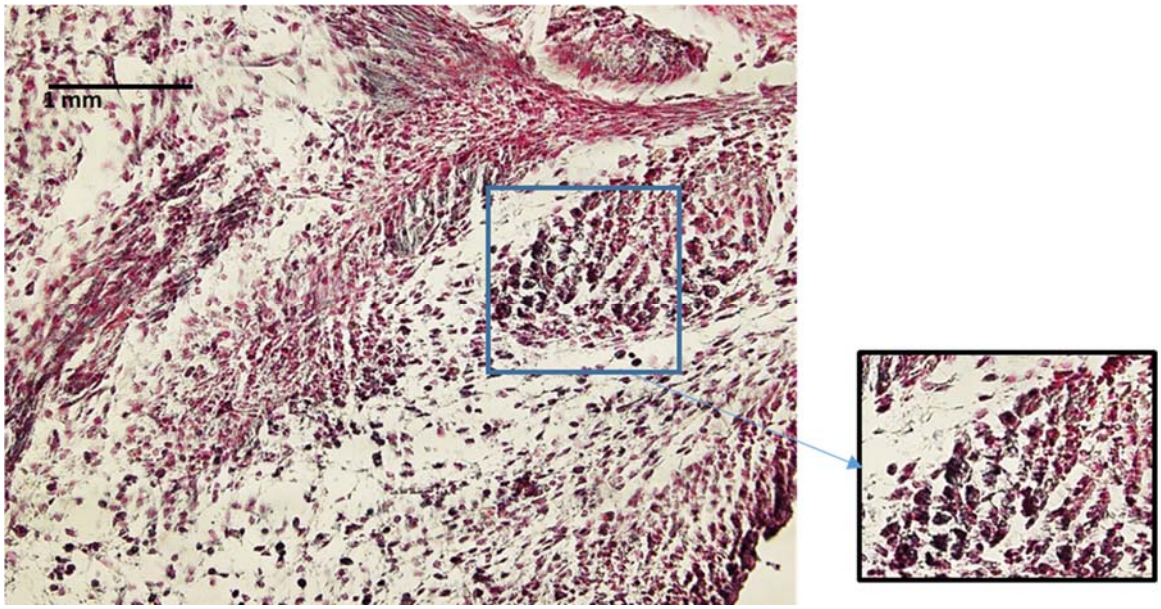

Figure 3.15 Bright field image of a section through a mouse embryo exhibiting some nuclear staining for RALDH 2. Positive antibody control. 20x magnification.

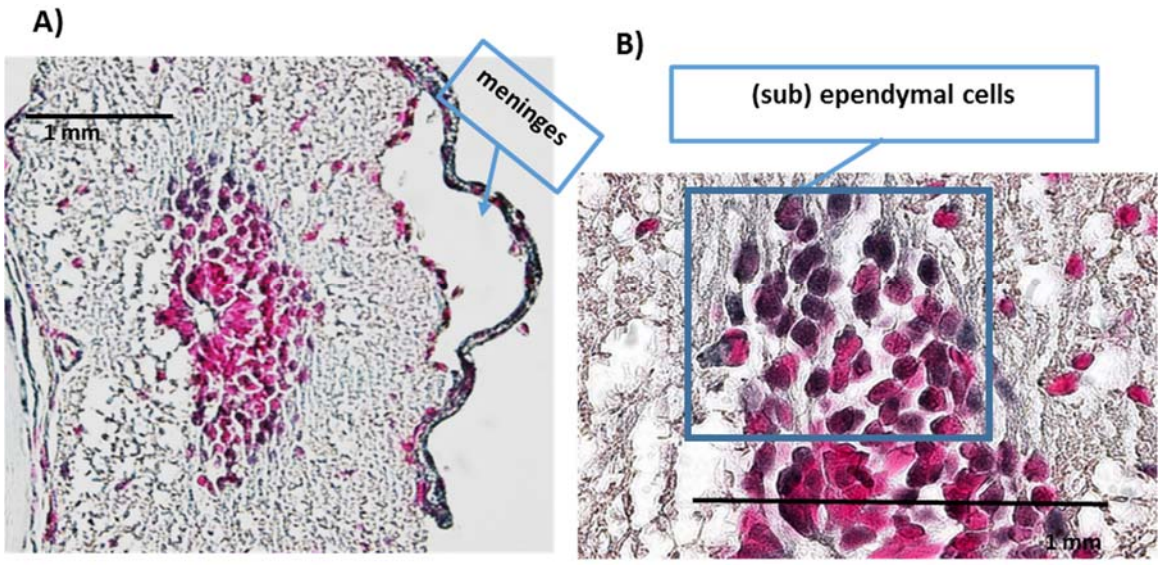

Figure 3.16 Bright field images of an intact cord section labeled with α-RALDH 2. Expression is present in the meninges as well as cytoplasm of grey matter and (sub) ependymal cells. Peroxidase/antibody stain in black; Nuclear fast red stain in red (nuclei). 20x (A) and 60x (B) magnification, respectively.

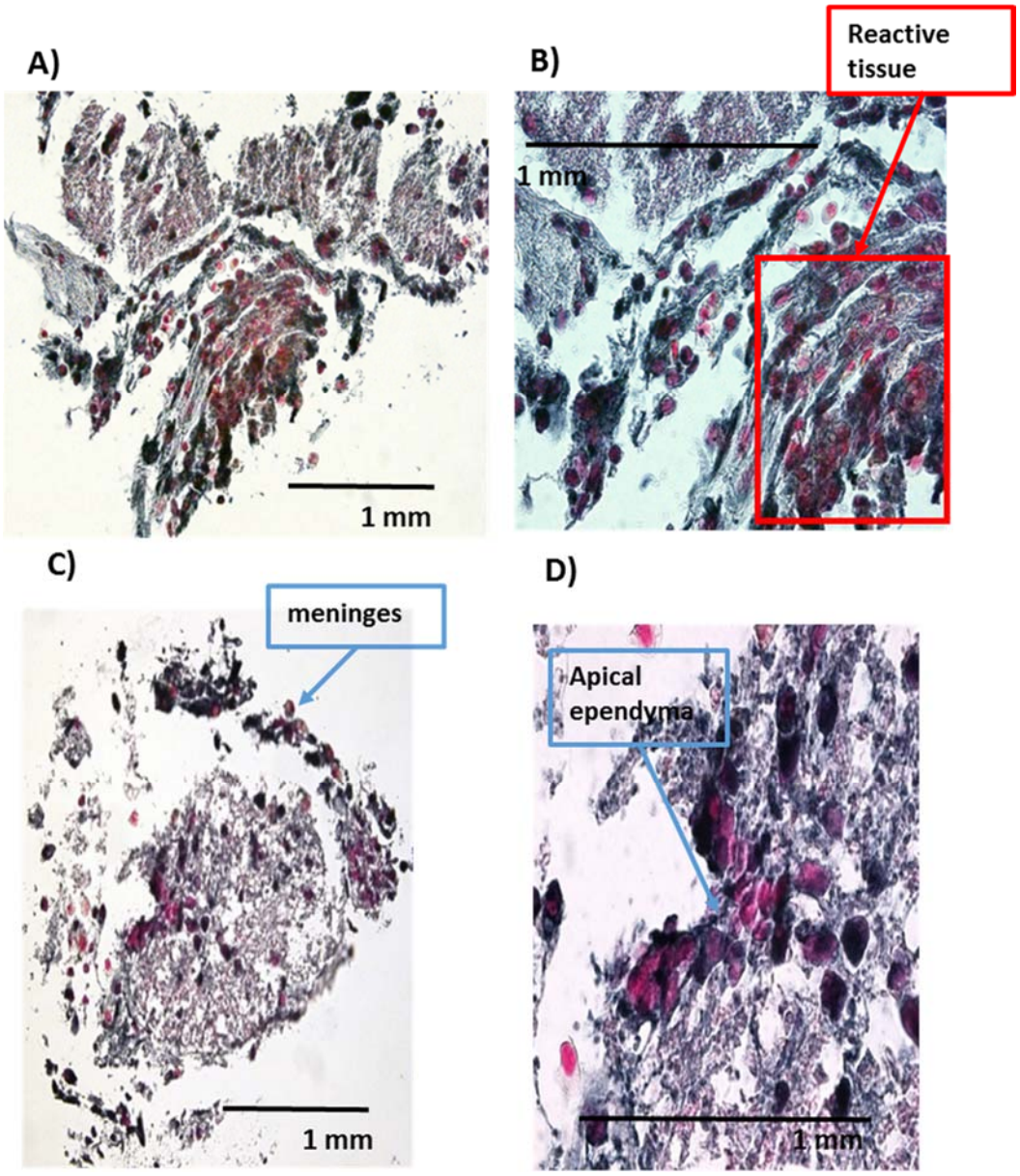

Figure 3.17 Bright field images of two week regenerate mesenchymal outgrowth (A and B) and reactive stump (C and D) sections labeled with α-RALDH 2. Cell outgrowth within the lesions site shows α-RALDH 2 localization. Within reactive stump sections, expression is present in the cytoplasmic and perinuclear regions of grey matter and ependymal cells as well as the meninges. Peroxidase/antibody stain in black; Nuclear fast red stain in red. 20x (A and C) and 40x (B and D) magnification, respectively.

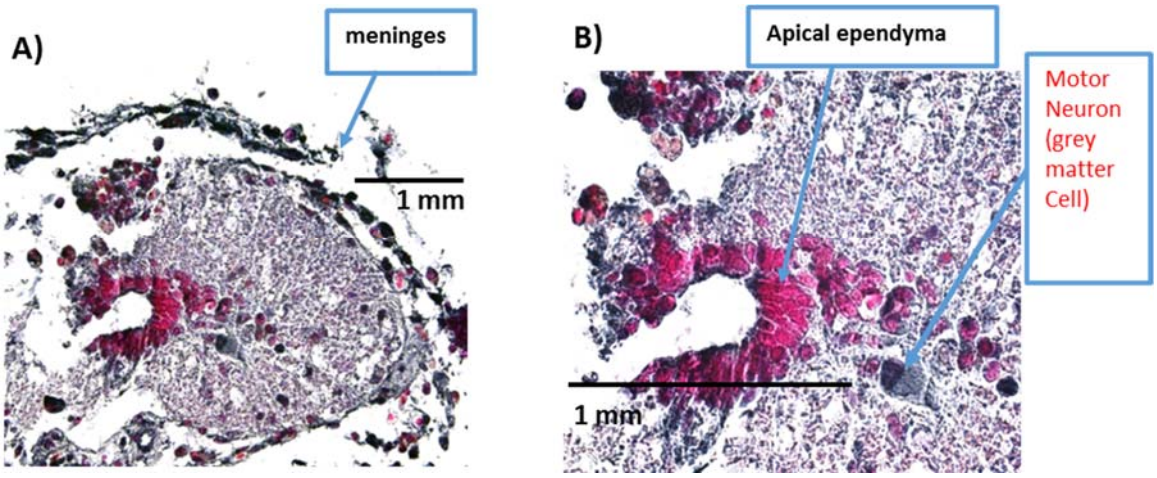

Figure 3.18 Bright field images of a two week regenerate stump section labeled with α-RALDH 2. Protein is present in the cytoplasmic and perinuclear regions of grey matter and apical ependymal cells as well as the meninges. Peroxidase/antibody stain in black; Nuclear fast red stain in red (nuclei). 20x (A) and 40x (B) magnification, respectively.

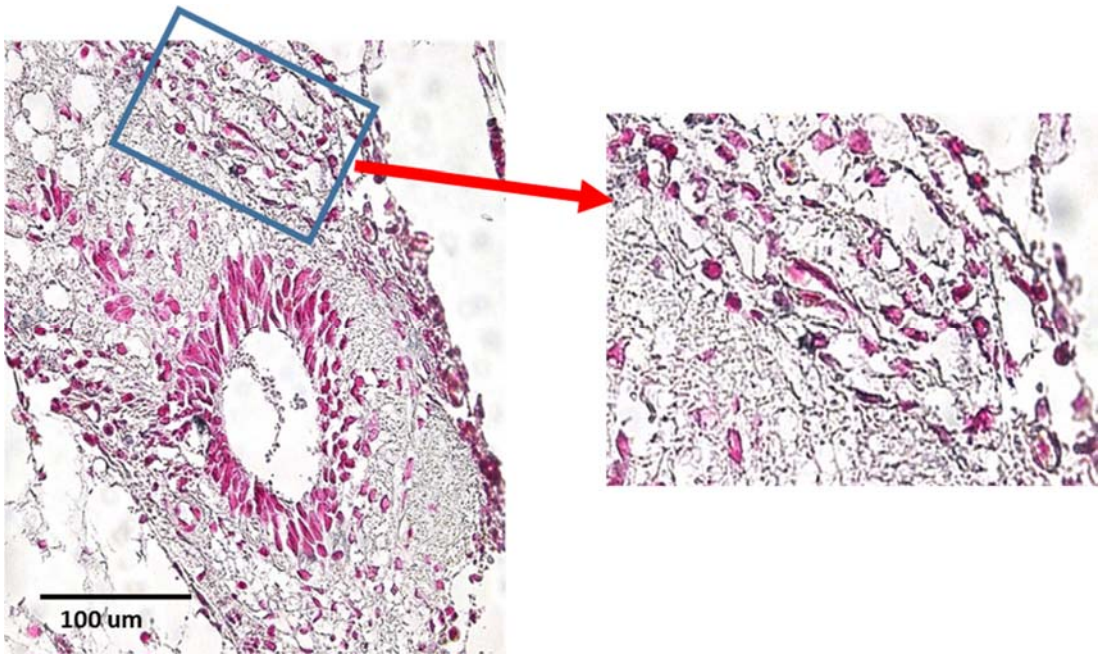

Figure 3.19 Bright field images of a five week regenerate stump section labeled with α-RALDH 2. Weak expression is present in the meninges; the fact that the meninges are expanded is indicative of continued reactivity during the later stages of the injury response. Peroxidase/antibody stain in black; Nuclear fast red stain in red (nuclei). 20x magnification.

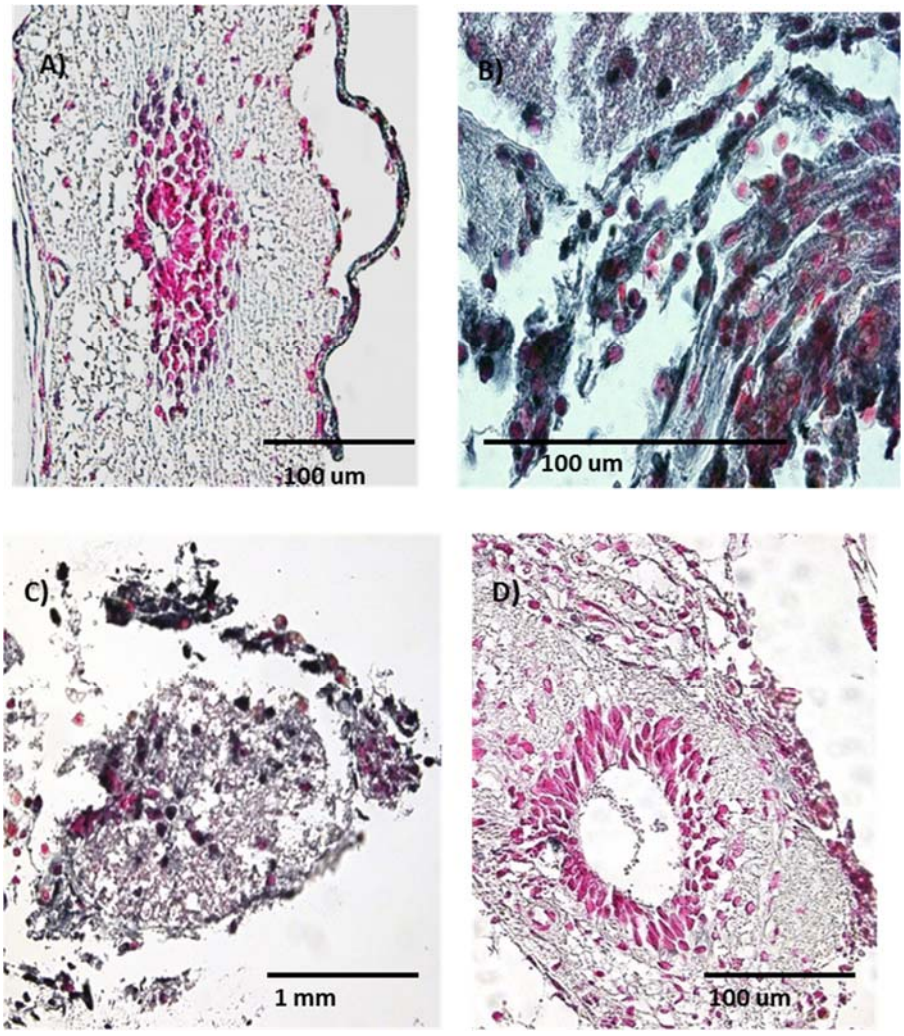

Figure 3.20 Summary of RALDH 2 expression. Intact cord (A). Two week regenerate cord (B). Two week regenerate cord stump (C). Five week regenerate (D).

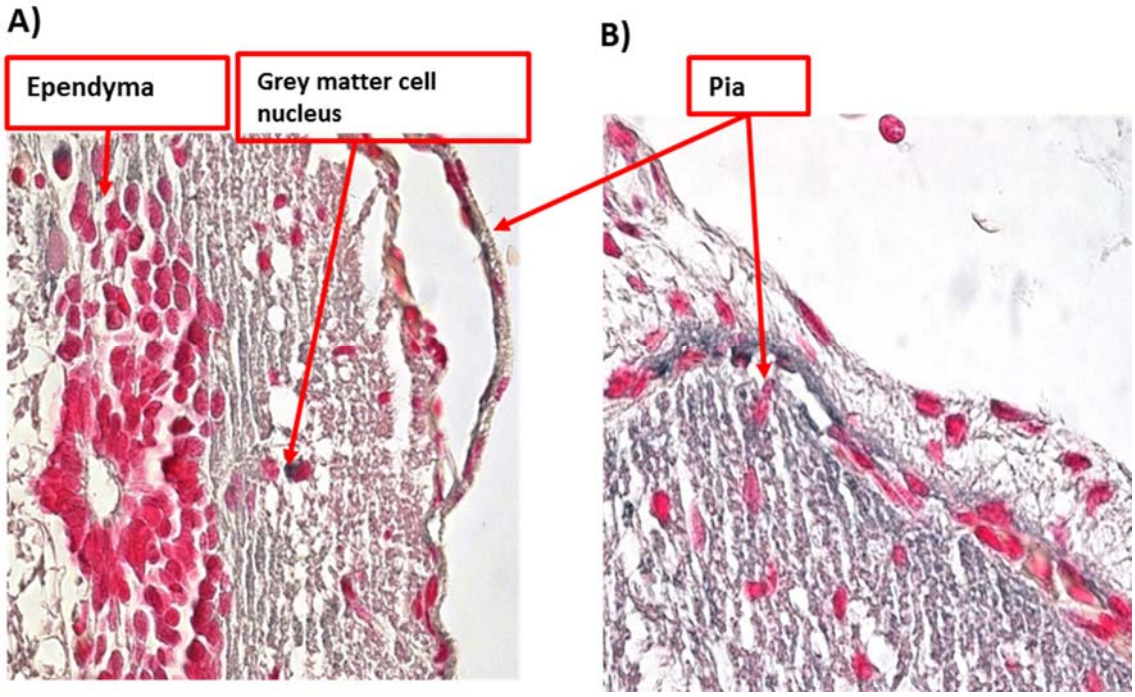

Figure 3.21 Bright field images of an intact cord section labeled with α-Sema 3A. Label is present in the cytoplasmic and perinuclear regions of gray matter cells as well as the leptomeninges. Peroxidase/antibody stain in black; Nuclear fast red stain in red (nuclei). 40x (A) and 60x (B) magnification, respectively.

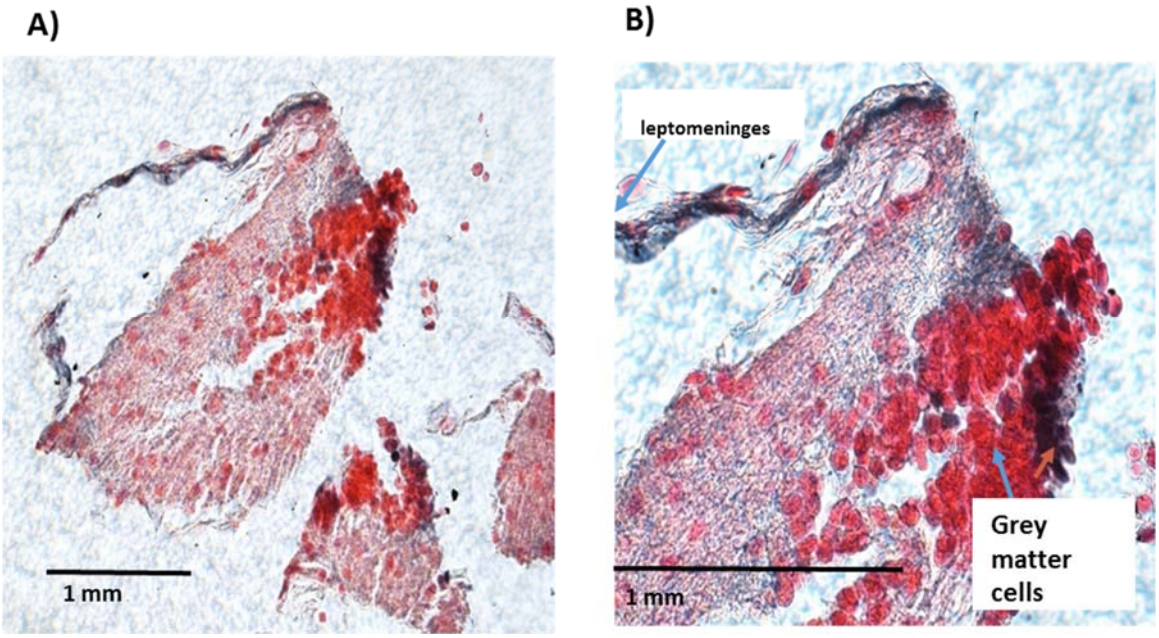

Figure 3.22 Brightfield images of a two week regenerate reactive stump cord section labeled with α-Sema 3A. Expression is present in the leptomeninges. Peroxidase/antibody stain in black; Nuclear fast red stain in red (nuclei). 20x (A) and 40x (B) magnification, respectively.

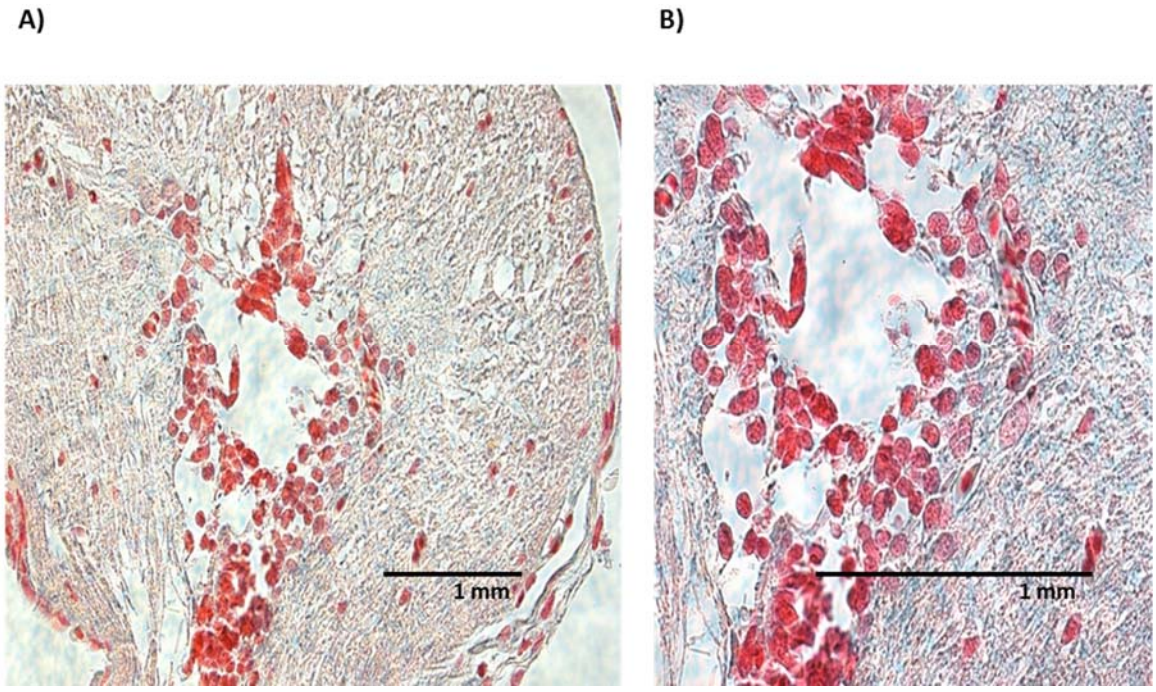

Figure 3.23 Brightfield images of a five week regenerate cord section labeled with α-Sema 3A. Label is absent in grey matter cell nuclei and is downregulated in the perinuclear and cytoplasmic regions of those cells as well as in the leptomeninges. Peroxidase/antibody stain in black; Nuclear fast red stain in red (nuclei). 20x (A) and 40x (B) magnification, respectively.

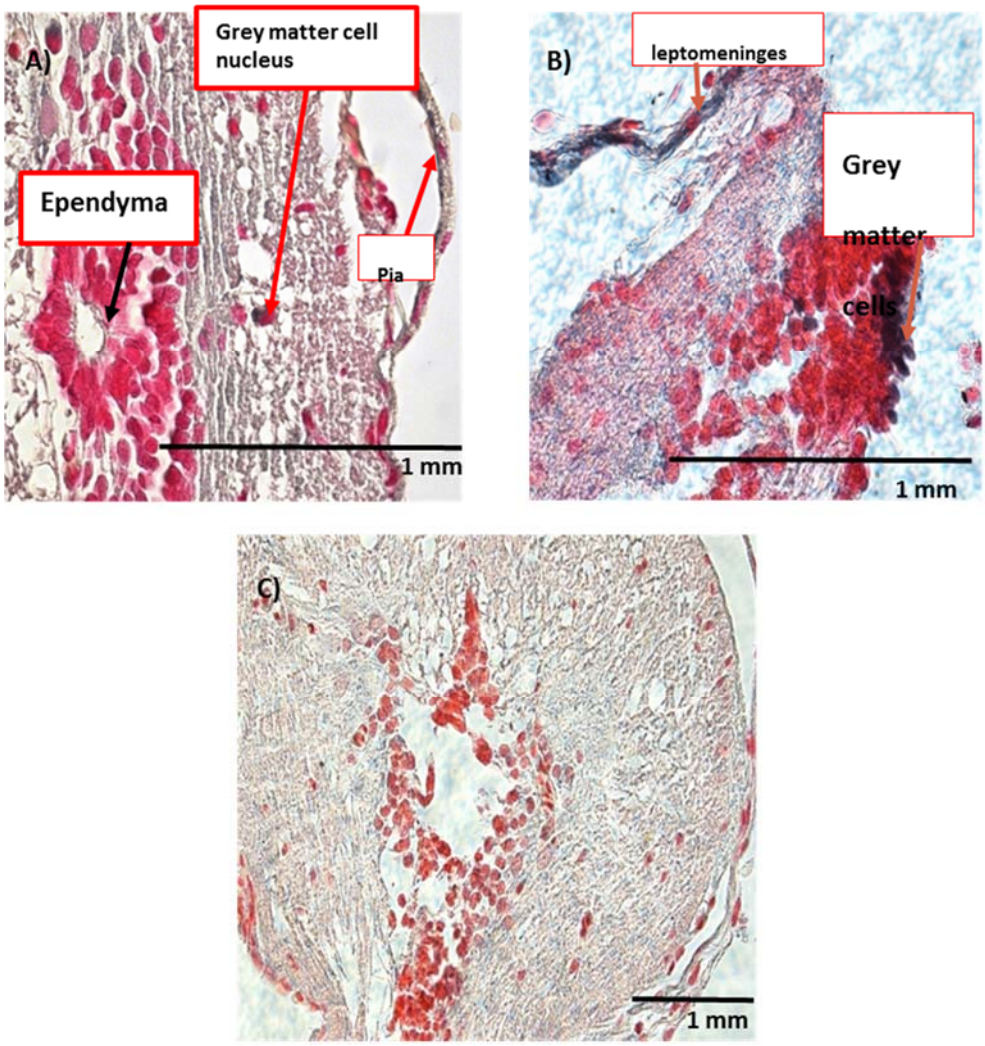

Figure 3.24 Summary of Sema 3A expression. Intact cord (A). Two week regenerate cord (B). Five week regenerate (C).

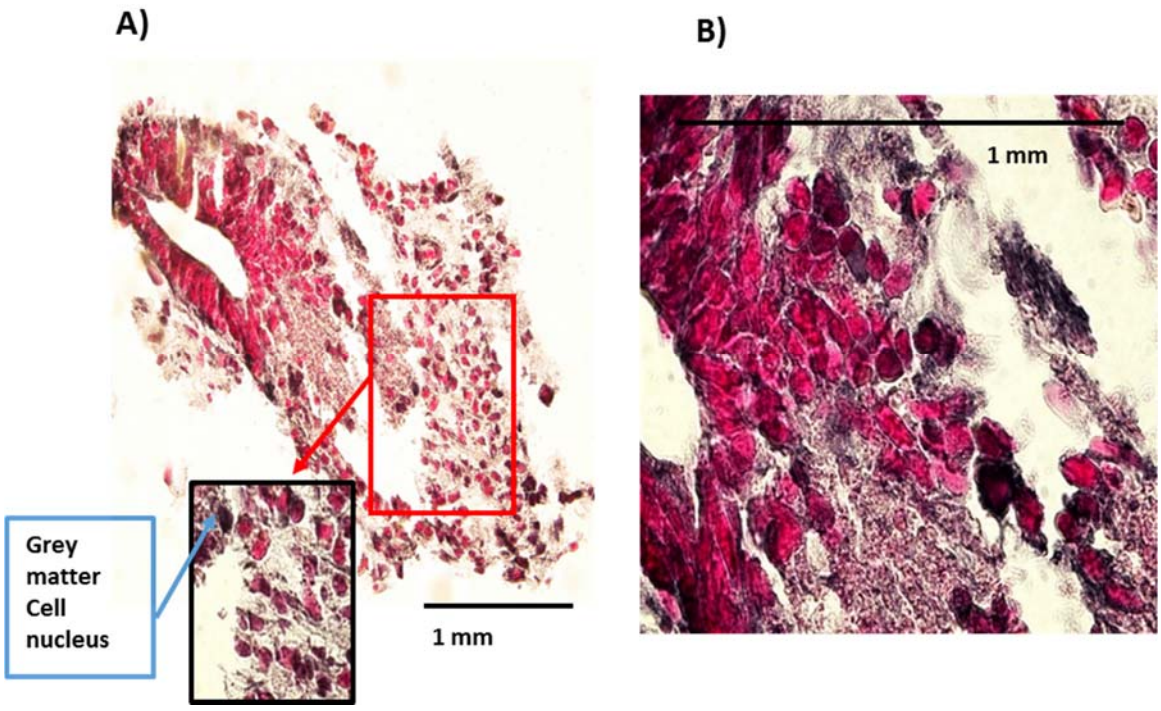

Figure 3.25 Bright field images of a two week regenerate fused cord section labeled with α-hMsi-1. Label is present in the cytoplasm of ependymal and some grey matter cells. Peroxidase/antibody stain in black; Nuclear fast red stain in red (nuclei). 20x (A) and 60x (B) magnification, respectively.

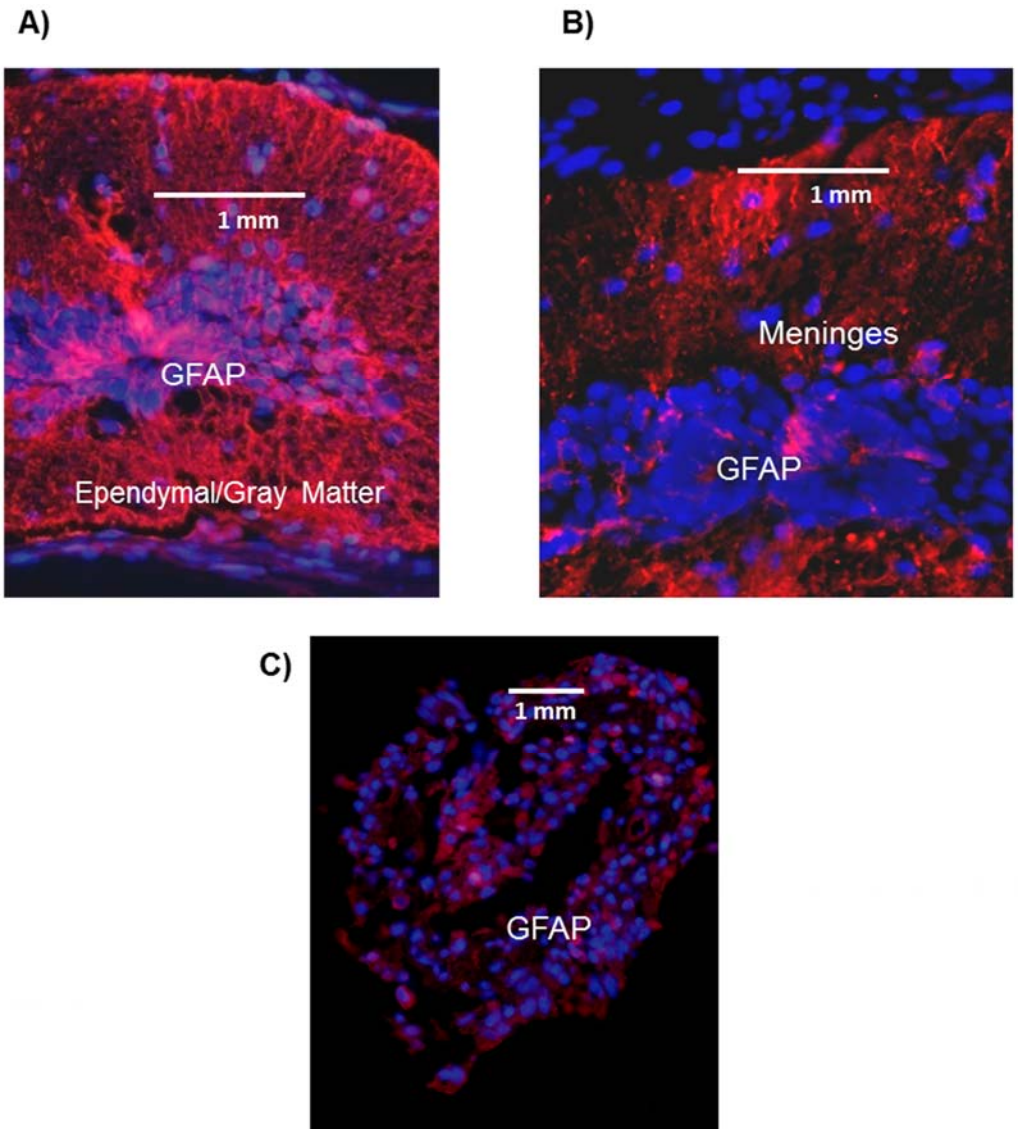

Figure 3.26 Epifluorescent images of sections labeled with α-GFAP intact cord (A), two week regenerate reactive stump cord (B), and mesenchymal ependymal outgrowth within the lesion site (C). In the intact cord, localization is present in ependymal cell processes and cell body cytoplasm; in the two week regenerate, expression is downregulated, indicating that the ependymal cells are degrading GFAP in response to injury. Finally, two week regenerate mesenchymal outgrowth shows small amounts of GFAP and no radial cell processes. Ependymal cell staining in red; DAPI nuclear stain in blue. 20x (A and B) and 10x (B) magnification, respectively.

Figure 3.27 Darkfield image of a whole mount two week regenerate cord stained with Alcian blue (proteoglycan stain) and Metanil yellow (collagen stain). The outgrowth at the lesion site shows a large concentration of red blood cells. 7x magnification

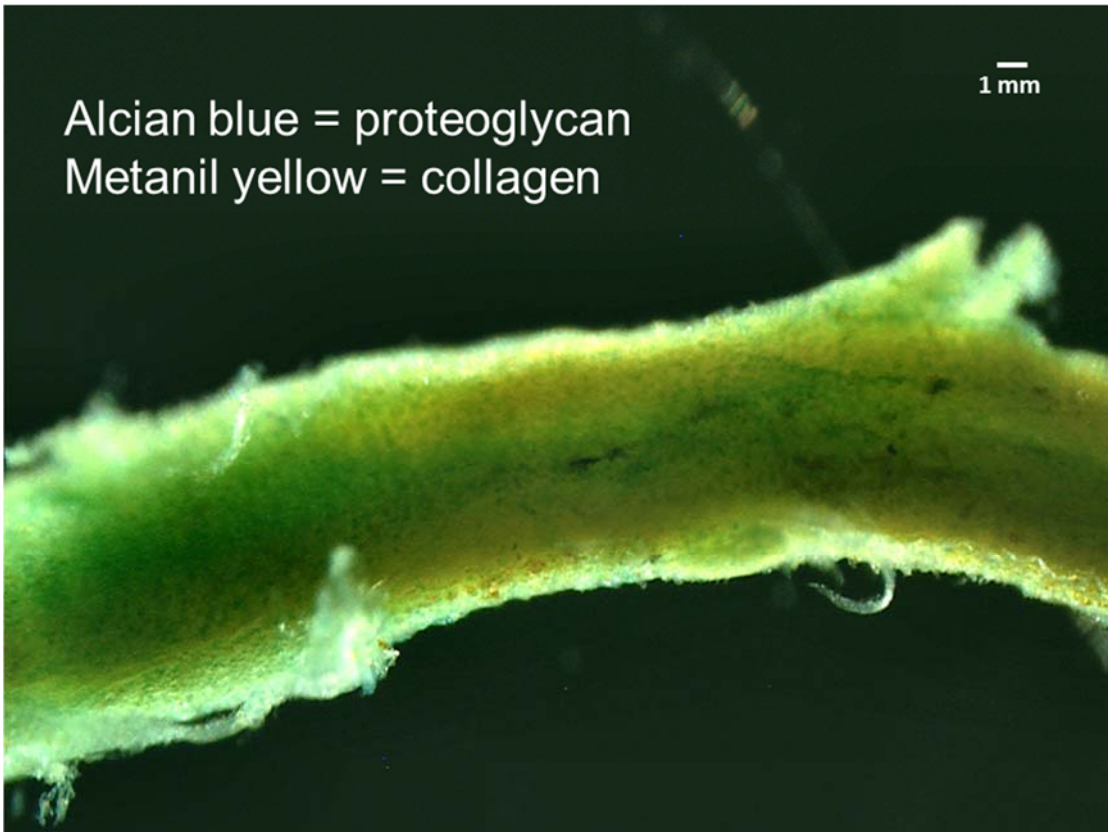

Figure 3.28 Dark field image of a whole mount two week regenerate cord stained with Alcian blue (proteoglycan stain) and Metanil yellow (collagen stain). The meninges at the lesion site contain a high concentration of proteoglycan. 4x magnification.

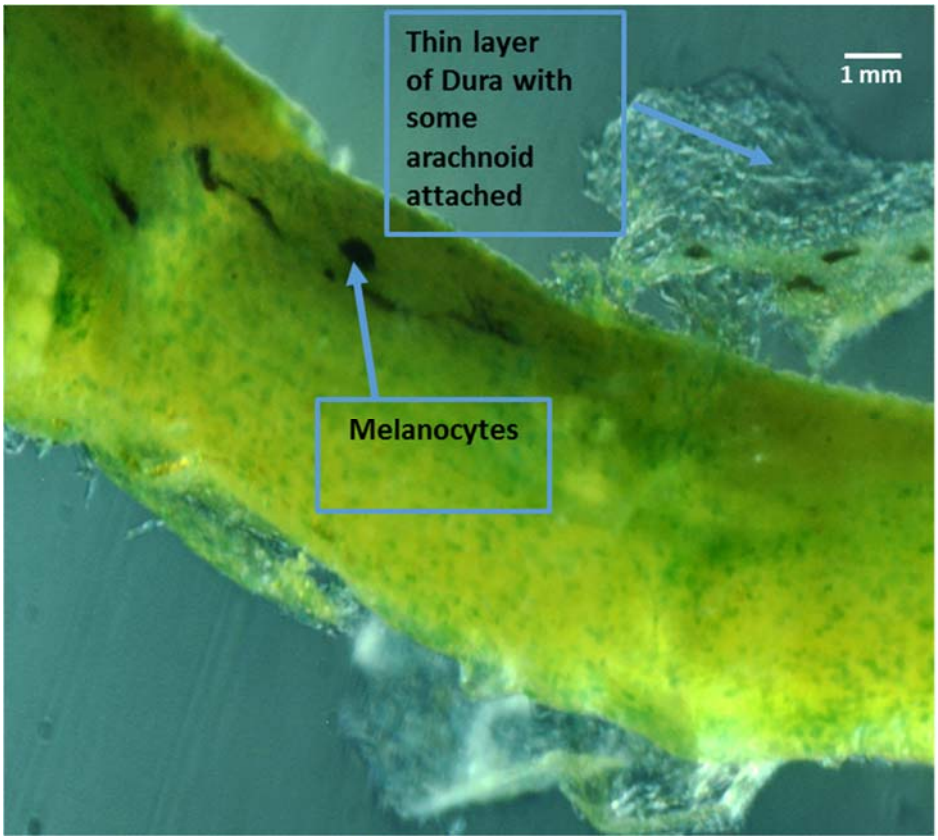

Figure 3.29 Dark field image of whole mount two week regenerate stump cord stained with Alcian blue (proteoglycan stain) and Metanil yellow (collagen stain). The meninges contain melanocytes, some proteoglycan and a significant amount of collagen. 7.5x magnification.

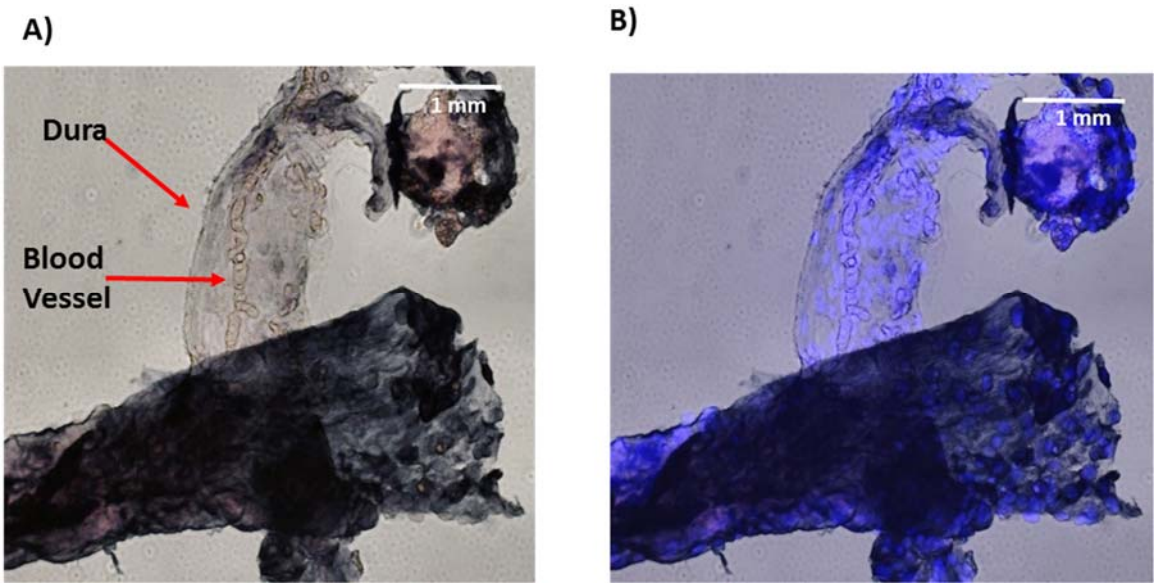

Figure 3.30 Dark field images of a whole mount two week regenerate cord labeled with CRABP 2. This protein is heavily expressed in the meninges. Peroxidase/antibody stain in black (A and B); DAPI nuclear stain in blue (B). 15x magnification.

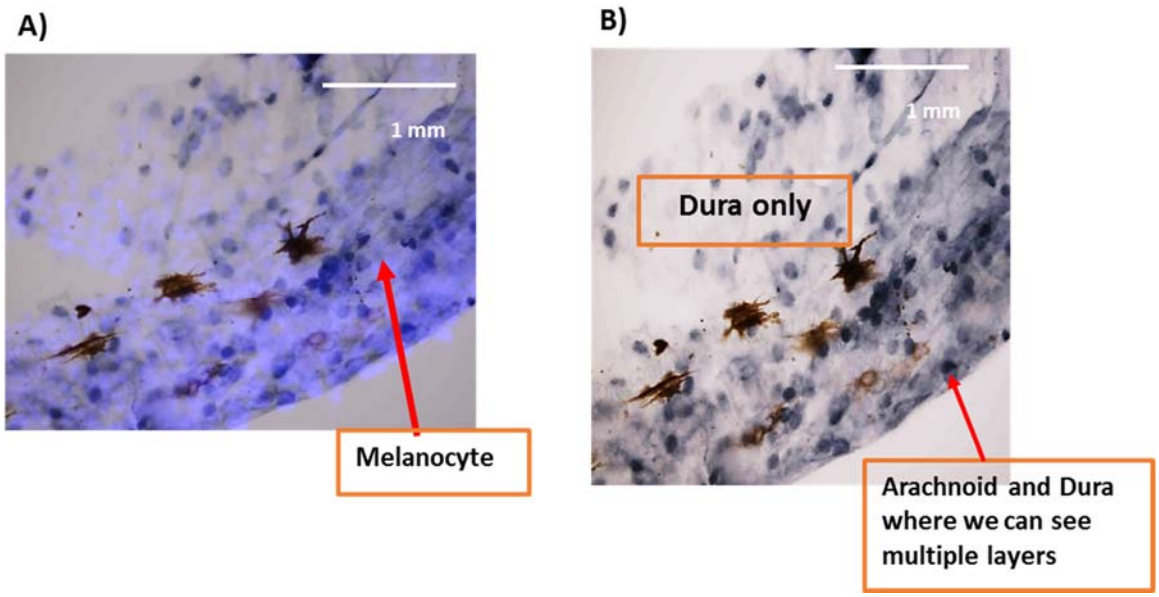

Figure 3.31 Dark field images of a whole mount two week regenerate cord labeled with RALDH 2. This protein is present in the meninges, which possesses many melanocytes, indicating that the respective expression is present in the arachnoid meningeal layer. DAPI nuclear stain in blue (A); Peroxidase/antibody stain in black (A and B). 20x magnification.

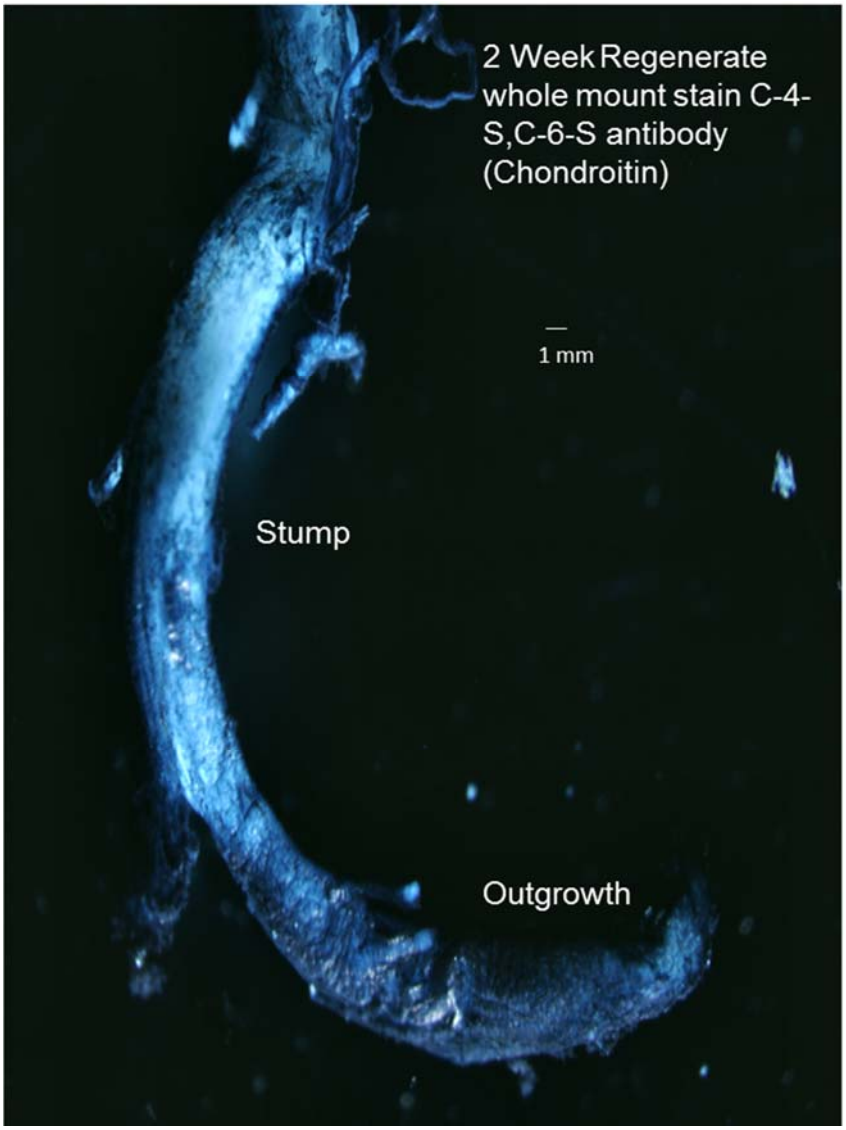

Figure 3.32 Darkfield image of whole mount Chondroitin -4-S and Chondroitin-6-S antibody peroxidase stained regenerating cord. Staining is strong at and near the tapered end, the region of cell outgrowth. 2.7x magnification.

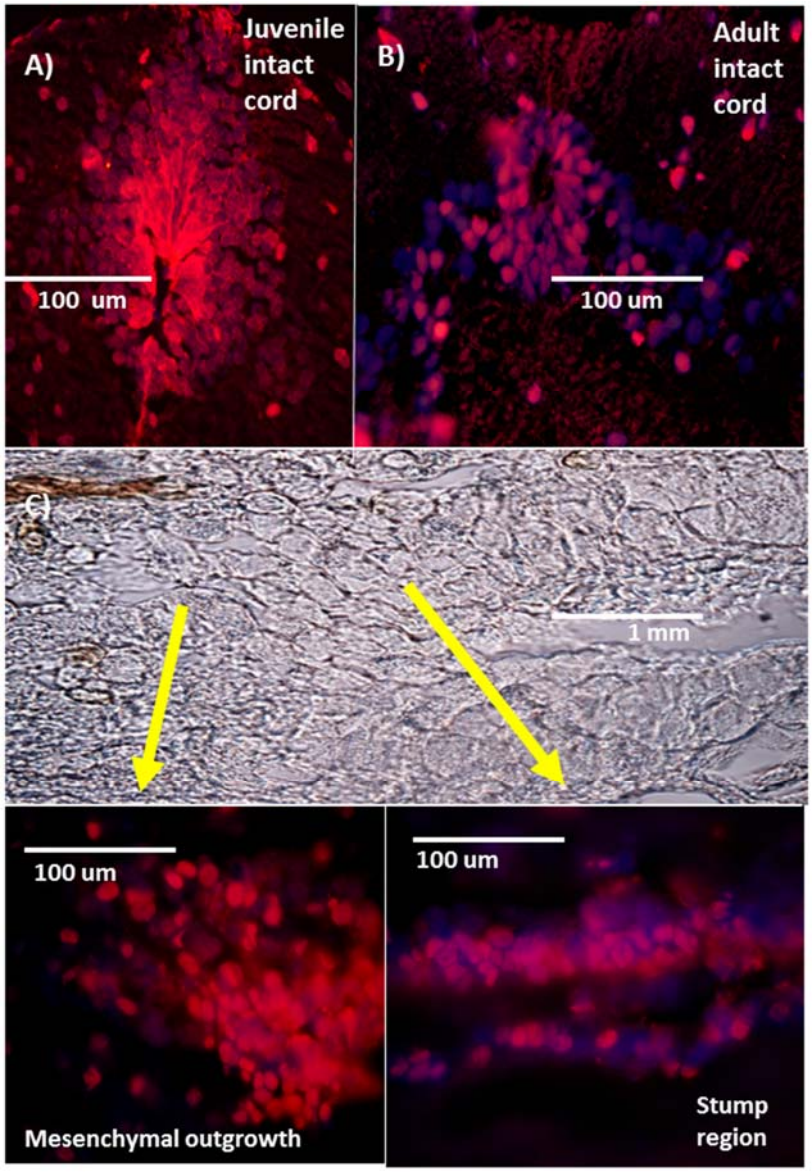

Figure 3.33 Fluorescent PCNA antibody labeling of juvenile (A) and adult (B) intact cords as well as two week regenerate cords (C). Red fluorescent signal indicates that in both tissue types the ependymal cells are mitotically active. A phase contrast image of the two week regenerate cord is included in C) as well. PCNA labeling in red; DAPI counterstain in blue. 20x magnification.

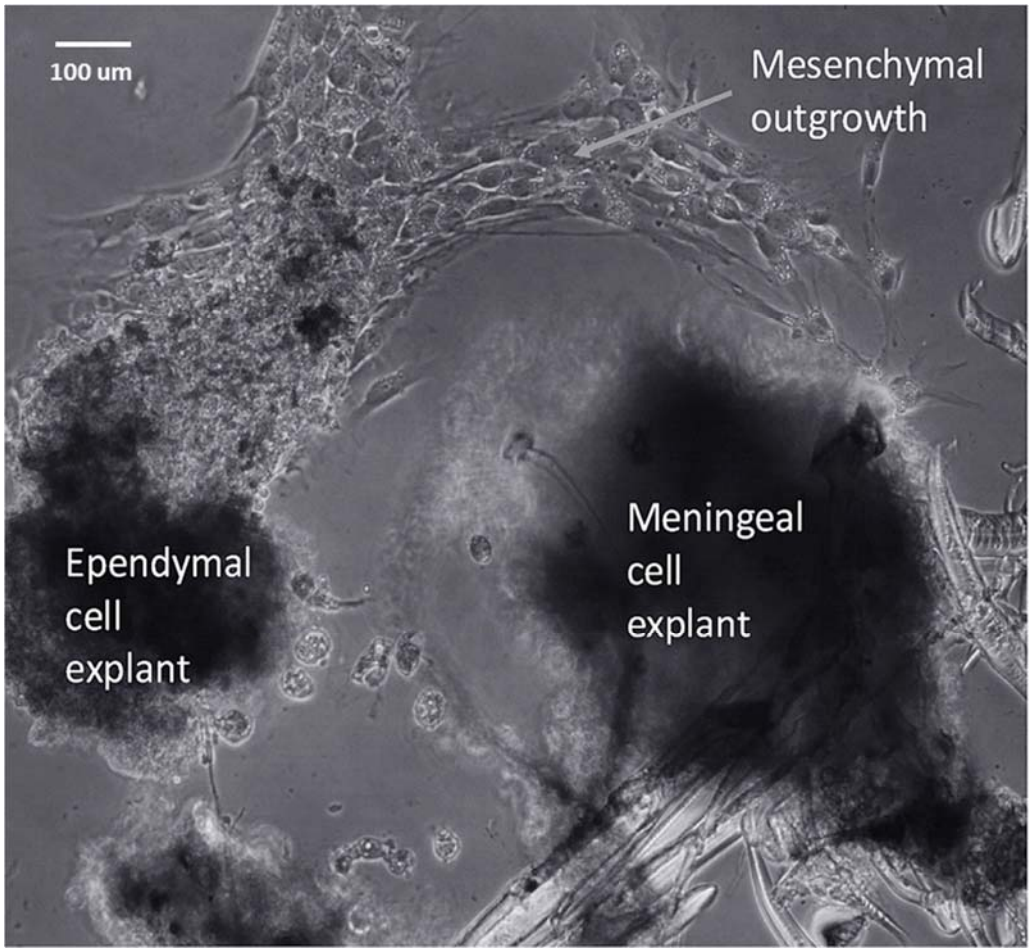

Figure 4.1 Phase contrast (converted to grayscale) image of a day five co-culture of ~14d regenerate ependymal (left) and meningeal (right) cell explants. Mesenchymal outgrowth is derived from the ependymal cell explant and migrates in the direction of the meningeal cell explant. 10x magnification.

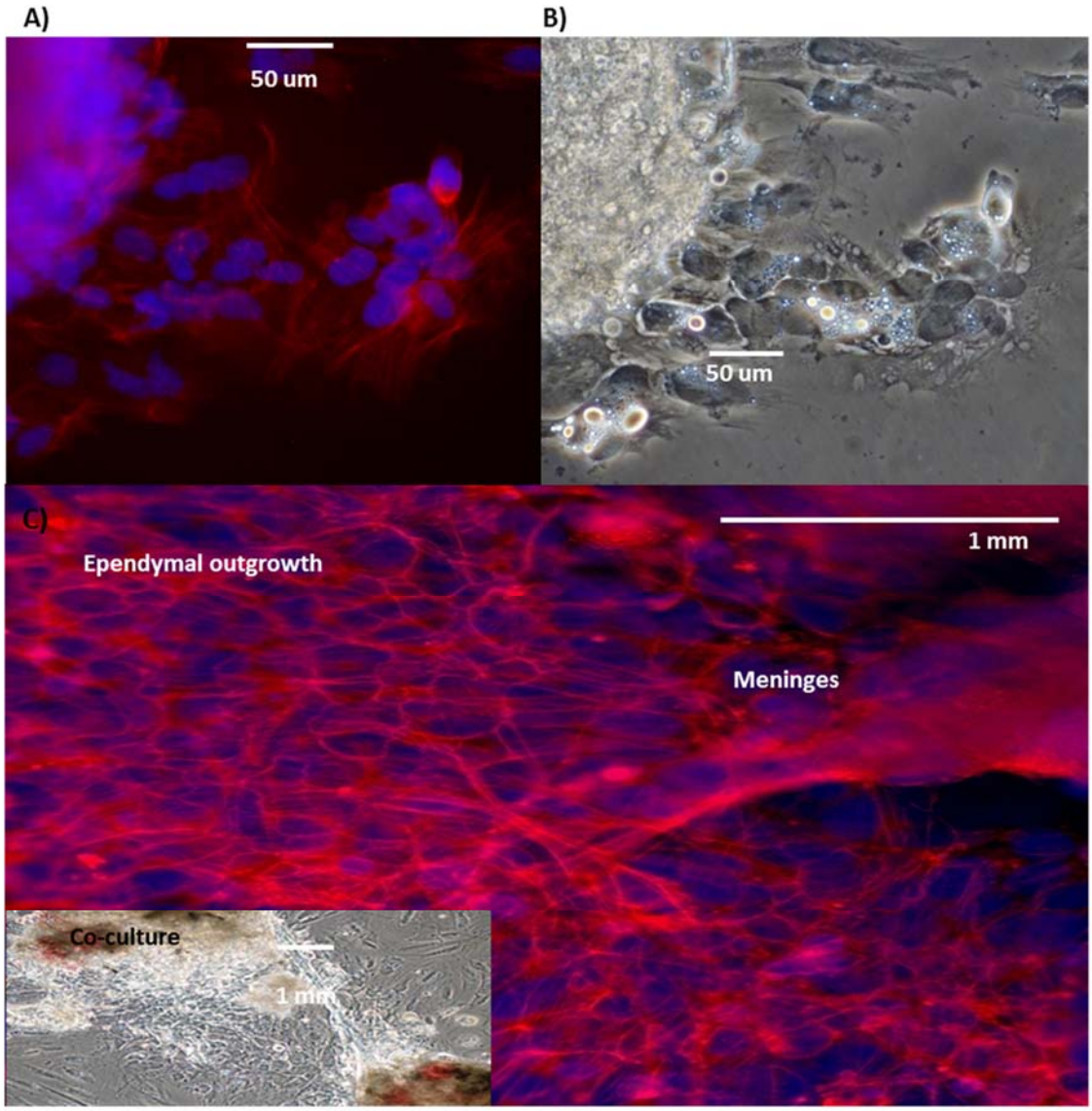

Figure 4.2 Epifluorescent (A) and phase contrast (B) images of a two week regenerate ependymal cell explant labeled with rhodamine-phalloidin. The elongated morphology of the F-actin labeled by the rhodamine-phalloidin probe indicates that mesenchymal ependymal cells are present. C) Fluorescent image of ependymal/meningeal co-culture (similar to that in figure 4.1). Rhodamin-phalloidin/DAPI stain shows honeycomb pattern of subapical actin microfilaments, indicating the re-epithelialization of the ependymal outgrowth in contact with reactive meninges. F-actin stain in red; DAPI nuclear stain in blue (A); Peroxidase/antibody stain in black (B). 30x (A), 50x (B), and 30x (C) magnification, respectively; 4x magnification of phase contrast inset in C).

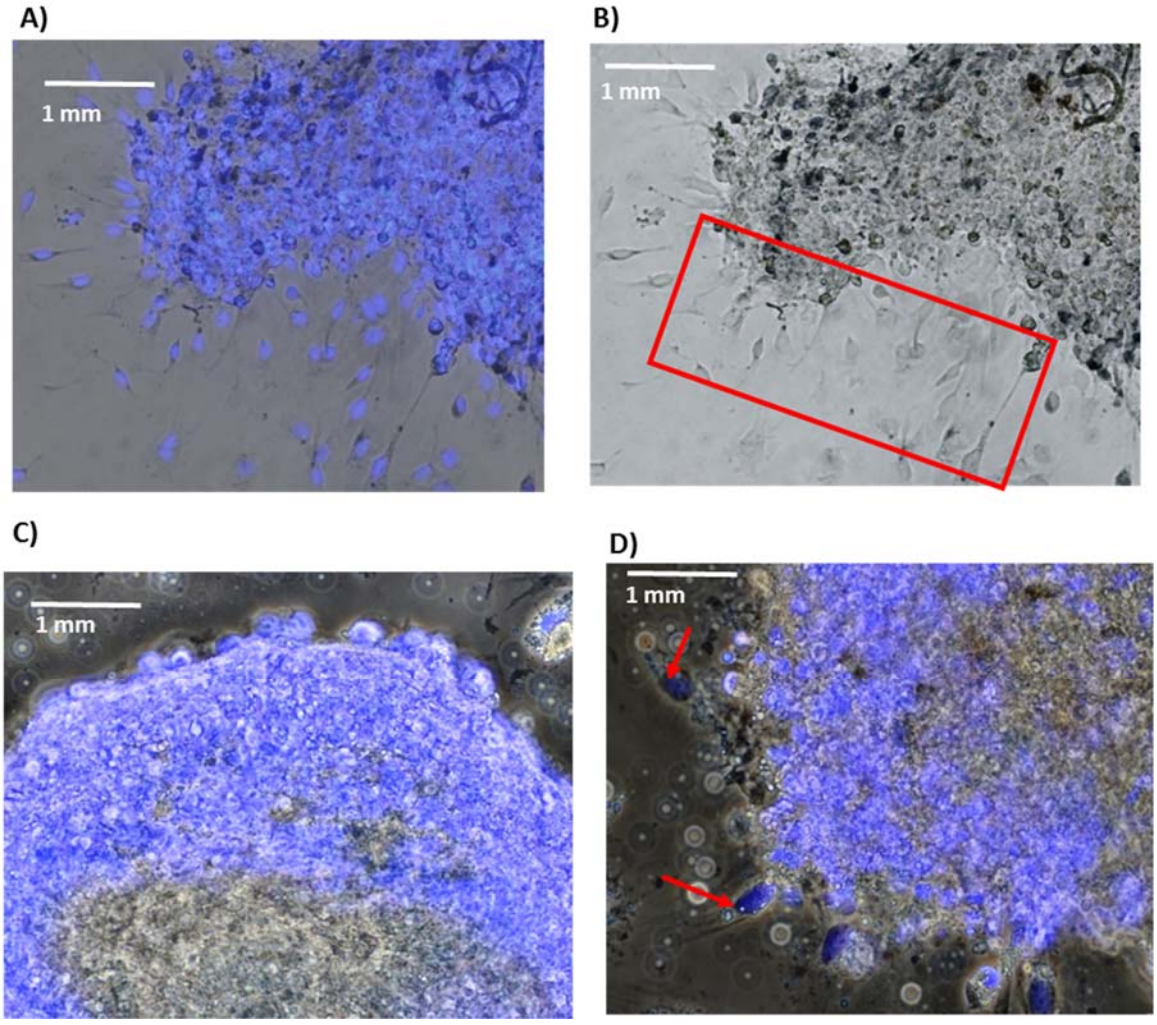

Figure 4.3 Epifluorescent (A, C, D) and phase contrast (B) images of two week regenerate meningeal tissue explants labeled with α-RALDH 2; mesenchymal ependymal cell outgrowth (remnants from the harvest, outlined in the box) is present in the periphery (B). Expression of this protein confirms respective presence of retinoids (A and B); the relative absence of mesenchymal outgrowth indicates that only meningeal tissue is present (C and D): the few mesenchymal cells present (arrows) are indicative of ependyma that did not get completely removed (D). DAPI nuclear stain in blue (A, C, D). 15x magnification.

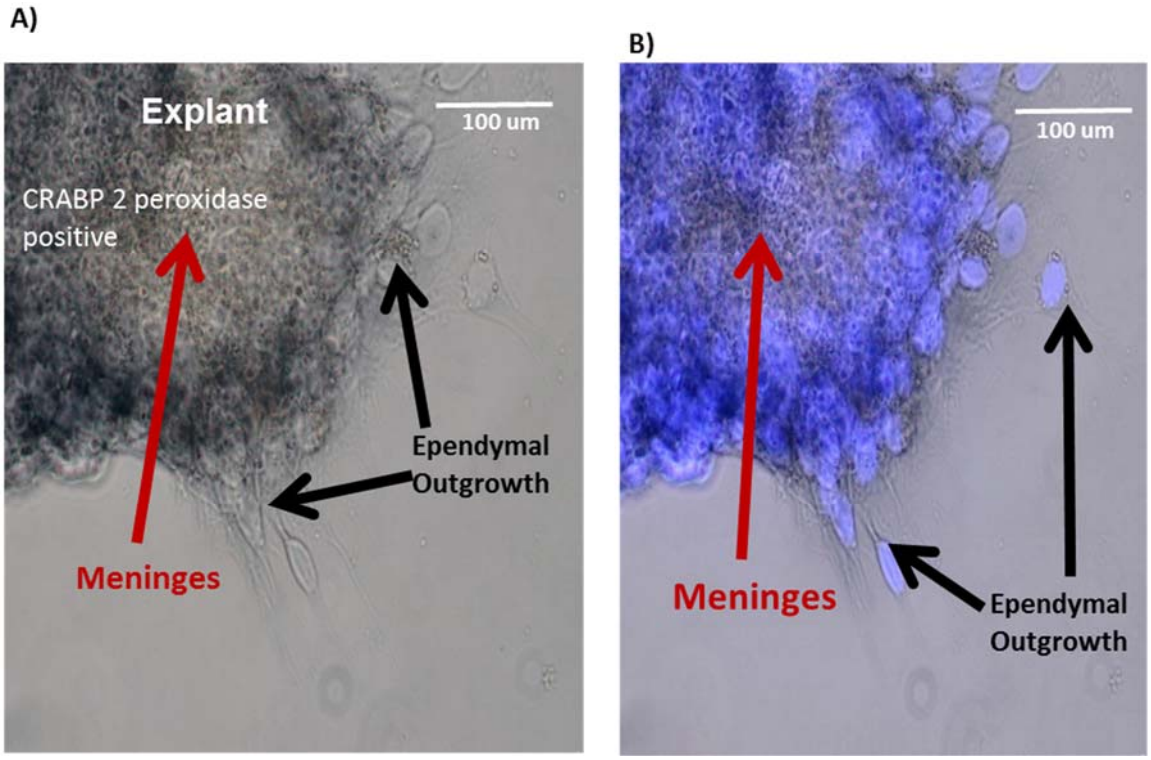

Figure 4.4 Brightfield (A) and epifluorescent (B) images of a two week regenerate meningeal/ependymal tissue explant labeled with α-CRABP 2. Both tissue types display expression of this protein. Peroxidase stain in black; DAPI nuclear stain in blue (B). 15x magnification.

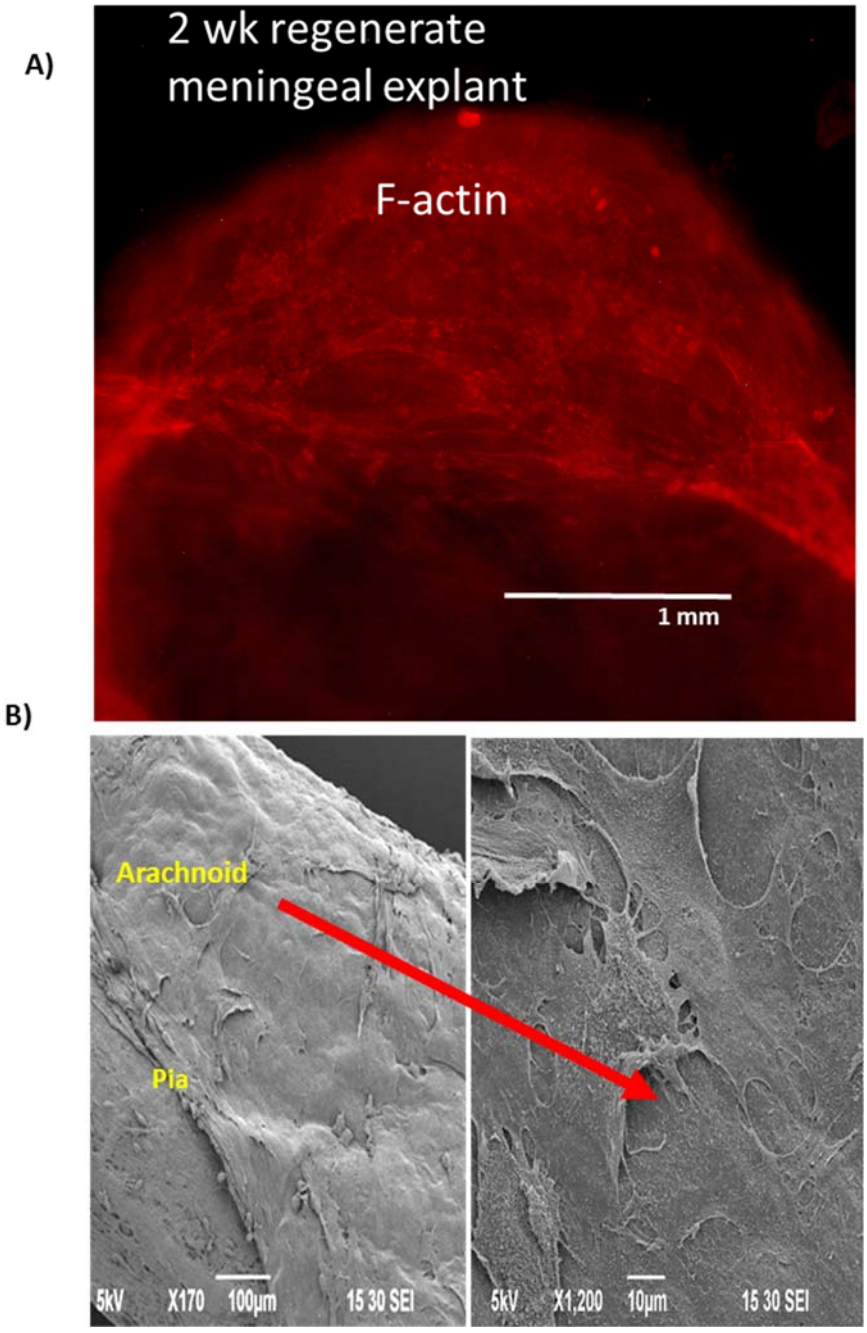

Figure 4.5 Rhodamine-phalloidin stain of a two week regenerate meningeal explant (A) displaying an F-actin pattern similar to that of the cell boundary pattern of the arachnoid of the adult intact meninges as identified by SEM (B). 30x magnification in (A). Magnification bars indicate 100µm and 10µm, respectively (B)

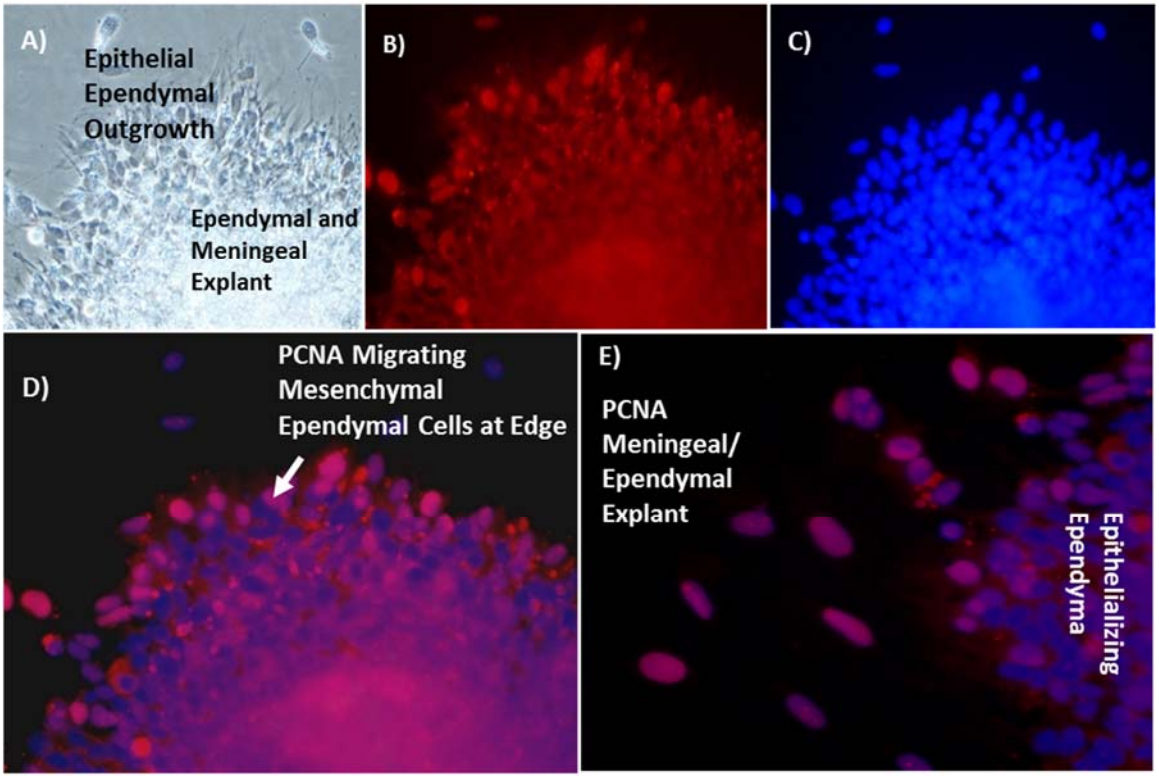

Figure 4.6 Day 7 phase contrast image of ependymal/meningeal tissue culture expressing PCNA, most notably where the mesenchymal ependymal cells are migrating from the edge of the explant (A). PCNA split-channel image (B). DAPI split-channel image (C). PCNA/DAPI overlay (D and E). Both epithelial and mesenchymal ependymal cells are both mitotically active. PCNA label in red; DAPI counterstain in blue. 20x (A-D) and 40x (E) magnification, respectively.